Chlorophyll triplet states in thylakoid membranes of *Acaryochloris marina*. Evidence for a triplet state sitting on the Photosystem I primary donor populated by intersystem crossing

Stefano Santabarbara[1,#*], Alessandro Agostini[2], Anastasia A. Petrova[1,§], Marco Bortolus[2], Anna Paola Casazza[3], Donatella Carbonera[2*]

[1] Photosynthesis Research Unit, Centro Studi sulla Biologia Cellulare e Molecolare delle Piante, Consiglio Nazionale delle Ricerche, Via Celoria 26, 20133 Milano, Italy.

[2] Department of Chemical Sciences, Università di Padova, Via Marzolo 1, 35131 Padova, Italy.

[3]Istituto di Biologia e Biotecnologia Agraria, Consiglio Nazionale delle Ricerche, Via Bassini 15a, 20133 Milano, Italy.

***To whom correspondence should be addressed**

S.S. Photosynthesis Research Unit, Consiglio Nazionale delle Ricerche, Via Bassini 15a, 20133 Milano, Italy. Tel: + 39 02 503 14857; e-mail: stefano.santabarbara@cnr.it

D.C. Department of Chemical Sciences, University of Padova, Via Marzolo 1, 35131 Padova, Italy. Tel: +39 498275144; Fax: +39 498275161; e-mail: donatella.carbonera@unipd.it

Present Addresses

[#]Istituto di Biologia e Biotecnologia Agraria, Consiglio Nazionale delle Ricerche, Via Bassini 15a, 20133 Milano, Italy.

[§]A. N. Belozersky Institute of Physical-Chemical Biology, Lomonosov Moscow State University, 119992 Leninskye Gory 1 building 40, Moscow, Russia.

Abstract. Photo-induced triplet states in the thylakoid membranes isolated from the cyanobacterium *Acaryocholoris marina*, that harbours Chlorophyll (Chl) *d* as its main chromophore, have been investigated by Optically Detected Magnetic Resonance (ODMR) and time-resolved Electron Paramagnetic Resonance (TR-EPR). Thylakoids were subjected to treatments aimed at poising the redox state of the terminal electron transfer acceptors and donors of Photosystem II (PSII) and Photosystem I (PSI), respectively. Under ambient redox conditions, four Chl *d* triplet populations were detectable, identifiable by their characteristic zero field splitting parameters, after deconvolution of the Fluorescence Detected Magnetic Resonance (FDMR) spectra. Illumination in the presence of the redox mediator N,N,N′,N′-Tetramethyl-p-phenylenediamine (TMPD) and sodium ascorbate at room temperature led to a redistribution of the triplet populations, with T_3 ($|D|=0.0245$ cm^{-1}, $|E|=0.0042$ cm^{-1}) becoming dominant and increasing in intensity with respect to untreated samples. A second triplet population (T_4, $|D|=0.0248$ cm^{-1}, $|E|=0.0040$ cm^{-1}) having an intensity ratio of about 1:4 with respect to T_3 was also detectable after illumination in the presence of TMPD and ascorbate. The microwave induced Triplet-minus-Singlet spectrum acquired at the maximum of the $|D|–|E|$ transition (610 MHz) displays a broad minimum at 740 nm, accompanied by a set of complex spectral features that overall resemble, despite showing further fine spectral structure, the previously reported Triplet-minus-Singlet spectrum attributed to the recombination triplet of PSI reaction centre, $^3P_{740}$ [Schenderlein M, Çetin M, Barber J, et al (2008) Spectroscopic studies of the chlorophyll *d* containing photosystem I from the cyanobacterium *Acaryochloris marina*. Biochim Biophys Acta 1777:1400–1408]. However, TR-EPR experiments indicate that this triplet displays an *eaeaea* electron spin polarisation pattern which is characteristic of triplet sublevels populated by intersystem crossing rather than recombination, for which an *aeeaae* polarisation pattern is expected instead. It is proposed that the observed triplet, which leads to the bleaching of the P_{740} singlet state, sits on the PSI reaction centre.

Introduction

Acaryochloris marina is an unusual cyanobacterium (Miyashita et al. 1996) which harbours Chlorophyll (Chl) *d* as the main chromophore bound to the core complexes of both Photosystem I (PSI) and Photosystem II (PSII). Chl *a*, that is otherwise the almost ubiquitously dominant pigment in the core complexes of oxygenic reaction centres (RC), is still present in *A. marina* with stoichiometries varying from 1-2 to 2-4 molecules per RC (Hu et al. 1998; Akiyama et a. 2002; Itoh et al. 2007; Tomo et al. 2007, 2008, 2011). The electronic transition of Chl *d* is about 15-20 nm red-shifted with respect to that of Chl *a* in organic solvents (Holt and Morley 1959; Nieuwenburg et al. 2007; Niedzwiedzki and Blankenship 2010). Similar red-shifts of the electronic transition are present in the Chl (*a*)/*d* binding protein complexes of *A. marina* (Schiller et al. 1997; Hu et al. 1998; Itoh et al. 2007; Tomo et al. 2008, 2011), with respect to those of the organisms in which Chl *a* is the predominant chromophore. The bulk, constitutive, replacement of Chl *a* with Chl *d* in *A. marina* can then be seen as an adaptive strategy to the environmental niche in which this organism strives, since it experiences substantial filtering of incident sunlight by other photosynthetic organisms, resulting in a large enhancement of far-red/near infrared radiation (Kühl et al. 2005).

Since Chl *d* represents more than 95% of the chlorophyll pool in this organism, this implies an average reduction of approximately 100 meV in the excited state energy at disposal for photochemical conversion. Such decrease in the maximal utilisable photon energy poses, in turn, ~~is~~ questions regarding the minimal energetic requirements for oxygenic photosynthesis, in conjunction with the efficiency of light conversion in photosystems operating with a lower energy headroom. For this reason, the role of the residual amount of Chl *a* present in both PSI and PSII of *A. marina* has been associated not only to light harvesting but also to photochemical and/or successive electron transfer (ET) reactions (Kumazaki et al. 2002; Schlodder et al. 2007; Itoh et al. 2007; Tomo et al. 2007, 2008, 2011; Ohashi et al. 2008; Renger and Schlodder 2008). Similar questions concerning the minimal energetic requirement for photochemical energy conversion apply also to a more recently discovered class of cyanobacteria that are capable of conditionally activating the synthesis of both Chl *d* and, to a larger extent, Chl *f*, an even further intrinsically red-shifted chromophore. The biosynthesis of long-wavelength absorbing Chls is elicited when these organisms are exposed to heavy filtering of incident radiation by other photosynthetic organisms and/or environmental factors, through the so called FaRLiP response

(Gan et al. 2014; Ho et al. 2017). Furthermore, the accumulation of Chl *d* and *f* is accompanied by a large reshaping of the photosynthetic apparatus involving the synthesis of specific isoforms of both PSI and PSII subunits as well as of the phycobilisome antenna. Yet, the maximal extent of Chl *d* and *f* accumulation is about 10% of the total Chl pool, so that Chl *a* remains always the dominant pigment in cyanobacteria capable of the FaRLiP response (Gan et al. 2014; Ho et al. 2017). Whereas the role of the intrinsically red-shifted Chl *d* and, especially, Chl *f* as antenna pigments upon the induction of the FaRLiP transition is generally accepted, their possible involvement in photochemical reactions in PSII (Allakhverdiev et al. 2016; Nürnberg et al. 2018; Mascoli et al. 2020; Zamzam et al. 2020) and especially PSI, remains controversial, since evidence both in favour (Kaucikas et al. 2017, Nürnberg et al. 2018) and against (Cherepanov et al. 2020, Kato et al. 2020) their participation in primary energy conversion has been presented. The very extensive and constitutive replacement of Chl *a* with Chl *d* in *A. marina* may then be understood as an extreme case of adaptation to incident light having a highly enriched component in the far-red portion of the spectrum.

The possible role of Chl *a* in the Chl *d*-dominated photosystems of *A. marina* and associated bioenergetic reconfigurations are briefly reviewed in the following paragraphs.

Photosystem I. In *A. marina* PSI clear evidence for the involvement of Chl *d* in photochemical conversion was originally gathered by transient optical spectroscopy at room temperature (RT) showing that the main bleaching associated with the oxidation of the terminal electron donor peaked at 740 nm, thereafter labelled as P_{740} (Hu et al. 1998). This is a remarkable red-shift with respect to the bleaching observed in canonical PSI, which falls at approximately 700 nm (Kok 1961; Ke 1973; Webber and Lubitz 2001), with subtle variations between species especially in the associated fine spectral structure (Witt et al. 2003; Nakamura et al. 2011). Further confirmation of the radical cation of P_{740} being located on Chl *d* molecules came from FT-IR (Sivakumar et al. 2003; Hastings and Wang 2008) and hyperfine-resolved electron paramagnetic resonance (EPR) spectroscopy (Mino et al. 2005) investigations. These evidences were later confirmed by structural models (Hamaguchi et al. 2021; Xu et al. 2021) showing a pair of Chl *d*/Chl *d'* (the latter being the epimer) molecules forming a dimer at the interface of the PsaA and PsaB reaction centre (RC) subunits, in analogy to Chl *a*/Chl *a'* composing P_{700}. Transient absorption measurements performed at low temperature (5-10 K) indicate that both the cation (P_{740}^{+}), under ambient redox conditions, and the triplet state ($^{3}P_{740}$), populated under

reducing conditions, display, even in place of significant differences in the satellite bands, a main bleaching at about 735-740 nm (Schenderlein et al. 2008) and hence likely involve either the same Chl(s) *d* giving rise to the differential absorption spectrum at RT, or a pool of Chls strongly interacting with them.

Surprisingly, the structural model of *A. marina* PSI identified the presence of Pheophytin *a* (Pheo *a*, the Chl *a* free base) at the so-called eC_3 position, in a symmetrical arrangement in both RC subunits (Hamaguchi et al. 2021; Xu et al. 2021). These cofactors, which are Chl *a* molecules in canonical PSI, can be identified with, or be part of, the so-called A_0 electron acceptor (reviewed in Brettel 1997; Santabarbara et al. 2005). The involvement of Pheo *a* in either primary charge separation or charge stabilisation reactions is consistent with the previous investigation by Kumazaki and coworkers (Kumazaki et al. 2002) which attributed a transient bleaching centred at approximately 680-685 nm to a Chl *a* acting as an electron acceptor. Since Pheo *a* has an intrinsically higher redox potential than Chl *a* by approximately 100-200 mV, depending on the solvent characteristics (Kobayashi et al. 2013), the substitution can be rationalised in terms of a compensation for the lower energy of the excited state, P_{740}^{*} with respect to P_{700}^{*}. This may explain the similarity in photon trapping kinetics reported for the isolated PSI of *A. marina* both by ultrafast transient absorption (Kumazaki et al. 2002) and fluorescence lifetime studies (Mi et al. 2003) with respect to Chl *a* binding PSI of other cyanobacterial species (reviewed in (Gobets and van Grondelle 2001).

The nature of the Chls in the so called eC_2 position, located between the P_{740} Chl *d* dimer and the Pheo *a* molecules, is less well established because of difficulties in assigning unambiguously the Chls at the current model resolution. Hence, although the authors assigned these molecules also to Chl *d*, there remains a possibility for Chl *a* being part of the RC.

The structure of *A. marina* PSI does not show any other significant differences in the arrangement of the other cofactors involved in electron transfer reactions. This is in agreement with previous functional spectroscopic studies indicating that the rate of charge recombination between P_{740}^{+} and either the reduced terminal iron-sulphur cluster acceptors $F_{A/B}$ (Hu et al. 1998) ~~and~~ or the semi-phylloquinones, A_1^{-}, both at RT (Hu et al. 1998) and at cryogenic temperatures (Schenderlein et al. 2008), were in line with those of canonical PSI. Only the kinetics of A_1^{-} oxidation by the successive acceptor, the iron-sulphur cluster F_X, appeared to be somewhat

slower (biphasic, 355 ns and 88 ns (Santabarbara et al. 2012)) than in canonical PSI (250-300 ns and 10-25 ns, for reviews see: Brettel 1997; Santabarbara et al. 2005, 2010). The similarity of both forward electron transfer (ET) and recombination kinetics therefore ~~to~~ indicates a substantial conservation of the energetic properties of the PSI acceptor side in *A. marina*, considering that the redox midpoint potential of the terminal donor P_{740}^{+} (Bailleul et al. 2008; Schenderlein et al. 2008) is also equivalent to that of P_{700}^{+}, *i.e.* + 425-460 mV (Nakamura et al. 2011). Besides the nature of the pigments composing the RC, the other main difference revealed by the structures between canonical PSI and that of *A. marina* is the reduced number of antenna molecules, with a total of about 75 Chl *d* in the latter with respect to about 90 Chl *a* in the former.

Photosystem II. The nature of the cofactors involved in photochemical reactions in *A. marina* PSII and, in particular, the specific role of Chl *d* have not been fully established yet. Nonetheless, evidence has been reported in favour of the primary electron donor being either Chl *d* or a Chl *d*/Chl *a* heterodimer (Schlodder et al. 2007; Renger and Schlodder 2008; Ohashi et al. 2008; Tomo et al. 2007, 2011). The mean excited state energy for the pigment constituting the RC has been on this basis estimated to correspond to a photon of between 713 nm (Tomo et al. 2007, 2011) 725 nm (Schlodder et al. 2007; Renger and Schlodder 2008; Itoh et al. 2007), that is about 15-30 nm red-shifted with respect to 685 nm in canonical Chl *a*-binding PSII. This is equivalent to a decrease of about 60-100 meV at disposal for photochemical reactions, a loss comparable to that experienced by *A. marina* PSI. Substantial compensation for the decrease in the RC excited state energy appears to be provided by a higher redox potential of the active Pheo *a* acceptor that has been titrated at about –480 mV in manganese depleted *A. marina* PSII (Allakhverdiev et al. 2010) that, after correction, would yield a potential of ~–410 mV for an intact core complex (Allakhverdiev et al. 2011). The Pheo *a* redox potential in the intact Chl *a*-binding PSII of *Synechocystis sp.* PCC6803 was determined to be –540 mV (Allakhverdiev et al. 2010) in a comparative study. On the other hand, only relatively subtle differences between the canonical PSII and the Chl *d*-dominated supercomplex of *A. marina* were observed for forward ET and recombination reactions between the quinone acceptors Q_A and Q_B and the donor side (Razeghifard et al. 2005; Renger et al. 2007; Cser and Vass 2007; Viola et al. 2022). Results from kinetic studies are in substantial agreement with direct redox titration of Q_A in manganese depleted PSII of *A. marina*, for which a corrected midpoint potential of ~ –70 mV was estimated

(Allakhverdiev et al. 2011), with respect to ~ –140 mV in Chl *a*-binding PSII. Based on the Pheo *a* titration data, the energy difference with Q_A would be therefore approximately 60 meV lower than in canonical PSII, but in both cases, larger than ~325 meV. The substantial, although not integral, conservation of the energetic properties of both the acceptor side and the cofactors involved in water splitting might be necessary for proton shuttling through the membrane and for chemical catalysis, respectively.

Light-induced damage of A. marina PSII. PSII embedded in the thylakoids of *A. marina* has been shown to be more susceptible to light-induced damage with respect to both canonical PSII and the Chl *a*/*f*-binding PSII of *Chroococcidiopsis thermalis* PCC 7203 (Viola et al. 2022), one of the best-characterised cyanobacterial strain displaying the FaRLiP response. The sensitivity of Chl-*d* binding PSII of *A marina* was shown to correlate with an enhanced light-induced singlet oxygen ($^1O_2$) sensitisation. This can be in principle rationalised by a larger propensity to populate the RC triplet state either due to the smaller energy gap between Q_A and Pheo *a* (Allakhverdiev et al. 2011, Viola et al. 2022) that shall facilitate the repopulation of the precursor radical pair from which the triplet originates, or to different, but yet to be established, energetics causing a marked increase of the lifetime of the $[P_{725}^{+}Pheo^{-}]$ radical pair precursor.

The study of the photo-induced triplet states in *A. marina* photosystems, particularly in a relatively intact environment such as the thylakoid membranes, can be helpful in understanding the role of Chl *d* and Chl *a* in photochemical reactions. The triplet states represent specific spectroscopic markers of the RC pigments, where the triplet population occurs, typically, through the charge recombination mechanism (for reviews see: Budil and Thurnauer 1991; Lubitz 2002). Although triplet-triplet migration can take place, it is a much slower process than singlet energy transfer, at least at low temperatures. The triplet state is then mainly localised on the chromophore on which it is initially populated, or nearby. The study of RC localised triplets, in turn, aids in the identification of the cofactors involved in charge separation reactions. Furthermore, Chl triplet states are known to be involved in light-induced photo-oxidative damage, especially to PSII (Durrant et al. 1990; Vass and Styring 1993; Telfer et al. 1994; Telfer 2014), since they can sensitise $^1O_2$ production via the interaction of O_2 that is a triplet ground state (Krasnovsky 1982, 1994; Krasnovskiĭ 2004). The energy level of ^{3}Chl *d*, albeit lower than that of ^{3}Chl *a*, is sufficient to interact with O_2 (Neverov et al. 2011; Hartzler et al. 2014). Singlet oxygen sensitisation is independent of whether the Chl triplet is populated via the recombination

mechanism in the RC or directly by intersystem crossing (ISC) from the singlet state. ISC is an active and significant decay pathway in Chls (Bowers and Porter 1967) that is typically considered to take place in light harvesting pigments. ^{3}Chl in the antenna are efficiently quenched by triplet-triplet energy transfer to carotenoids (Car). The Car triplet is too low in energy to interact with oxygen and hence, this state can decay harmlessly to the ground state (Wolff and Witt 1969; Mathis et al. 1979; Kramer and Mathis 1980; Siefermann-Harms 1987). Nonetheless, even residual or imperfect quenching by Car, can lead to the presence of potentially harmful ISC populated ^{3}Chl (Santabarbara et al. 2001, 2002b; Santabarbara and Jennings 2005).

The triplet population mechanisms can be discriminated performing time-resolved EPR (TR-EPR) experiments, since the spin polarisation pattern of the light-induced EPR spectrum of ^{3}Chls is *eeeaaa or eaeaea* for ISC and *aeeaae* for the recombination mechanism (Budil and Thurnauer 1991; Lubitz et al. 2002). EPR spectroscopy also allows to estimate key features characterising the triplet state, such as the zero field splitting (zfs) parameters, that ~~often~~ depend on the chemical nature of the cofactor but can also be modulated by the surroundings that provide solvation and coordination.

On the other hand, most EPR approaches do not give any direct information on the optical properties of the cofactors carrying the triplet state. A notable exception is represented by Optical Detected Magnetic Resonance (ODMR) in zero-magnetic field, a technique that allows to directly detect the changes in the optical properties of a system due to the change in triplet populations, elicited by resonant microwave frequencies between a couple of triplet sublevels. ODMR is intrinsically a bi-dimensional technique, providing a microwave spectrum when monitoring at a fixed observation wavelength, and an optical ~~spectrum, most commonly,~~ Triplet-minus-Singlet (TmS) spectrum, when sitting at a resonance frequency and scanning the observation wavelength. ODMR has superior resolution for zfs determination compared to EPR, because of the absence of an applied magnetic field, allowing to resolve triplet populations which would be otherwise indistinguishable by EPR, and to simultaneously characterise their associated optical properties (Carbonera 2009). Hence, both ODMR at 1.8 K and TR-EPR (between 10 and 100 K) were here applied in order to characterise the photo-induced Chl triplets in the photosystems embedded in the thylakoid membrane of *A. marina*.

Materials and Methods

Growth conditions. *A. marina* cells were cultivated in a modified BG11 medium, in which distilled water was replaced by artificial sea-water (SW-BG11). Cells were initially grown in 250 mL and, when necessary, transferred to 1 L cylindrical flasks, containing 150 and 650 mL of liquid medium, respectively. In both cases the cultures were maintained under continuous aeration (4 L/min) and illumination, provided by 15 W incandescent lamps, giving an average photon flux density of 35 μmoles of photon m^{-2} sec^{-1} at the sample level, in a temperature-controlled room at 21 °C.

Thylakoid membranes purification. Cells were harvested by centrifugation at 9700x*g* for 5 min in a SS34 rotor (Sorvall), washed in 50 mM HEPES/NaOH pH 7.5 under the same centrifugation conditions and the pellet suspended in the same buffer. For thylakoid membranes preparation, 1-1.2 g of cells were disrupted using a TissueLyzer (Qiagen) in the presence of 212-300 μm glass beads (cells to beads ratio ~1:2). ε-aminocaproic acid and phenylmethylsulfonyl fluoride (PMSF) were used as proteases inhibitors. Broken material was first filtered through Mylar cloth and residual cell debris and glass beads were further removed by centrifugation (11150x*g* for 5 min). The resulting supernatant was centrifuged at 140000x*g* in a 50.2Ti rotor (Beckman) for 45 min and the pellet, containing the thylakoid membranes was suspended in a small volume of 50 mM HEPES/NaOH buffer (pH 7.5), frozen in liquid nitrogen and stored at –80 °C until use. Pigments concentration in thylakoids was estimated by pure methanol extraction using the extinction coefficient of 63.69 mg/mL at 697 nm (Li et al. 2012) in an Uvidec 510 (Jasco) spectrophotometer. All procedures were performed at 4 °C and under dim light or darkness.

Measurement conditions. Immediately before measurements, the sample was diluted to a final concentration equivalent to 100 μg mL^{-1} Chl *d* in a buffer containing 150 mM HEPES/NaOH buffer (pH 7.5), 100 mM KCl, 5 mM $MgCl_2$, and a final concentration of 60% v/v of glycerol to obtain a transparent glass at low temperature. For treatments with redox mediators (at the appropriate conditions as further reported in the text and figures), freshly prepared solutions of the reagents, N,N,N′,N′-Tetramethyl-p-phenylenediamine (TMPD), sodium ascorbate and sodium dithionite, were initially added to the concentrated thylakoid suspension, in the absence of glycerol, and incubated in the dark, on ice, for at least 15 minutes, after which a buffered mediators-containing glycerol solution was added to the samples to reach the final

desired ratio of cryoprotectant/water. All buffers and mediator solutions were degassed and flushed with nitrogen before use.

Sample illumination was performed using a 150 W projector, filtered through 10 cm of water and a heath mirror (Ealing 35-6865). Illumination was either performed at RT or at 77 K, by immersing the sample in an unshielded Dewar vessel.

Dark adapted and pre-illuminated samples were then immediately transferred to a pre-cooled cryostat at 60 K for ODMR measurement or frozen in liquid nitrogen in the measuring tube for EPR measurements.

Optically Detected Magnetic Resonance Apparatus. ODMR experiments were performed in a home-built apparatus which has been previously described in detail (Carbonera et al. 1992; Santabarbara et al. 2002a; Agostini et al. 2018), with some modifications. In brief, the amplitude modulated microwave field, generated by a HP8559b sweep oscillator equipped with the HP83522a plug-in device, by a Sco-Nucletudes 10-46-30 TWT amplifier was transmitted trough a semi-rigid coaxial cable to the sample held in a slow-wave helix with a pitch of about 2 mm, acting as broad band resonator. The experiments were performed with a maximum output power of 500 mW. The amplitude modulation frequency was set, if not otherwise differently indicated, at 33.3 Hz, and selected in order to maximise the ms-lifetime Chl triplet signals.

Optical excitation was provided by a 250 W tungsten lamp (Philips) led by a stabilised power supply. For fluorescence-detected measurements (FDMR) the sample was excited by a combination of broadband filters, consisting in a solution of $CuS0_4$ 0.1 M (path-length 5 cm), and a heath mirror (Ealing). The light was focused onto a flat cell (5,0 x 1,2 mm) placed in a liquid helium cryostat (Oxford instruments, mod. Spectromag 4) which was pumped to reach the operating temperature of 1.8 K. The sample was kept with the normal to its plane rotated 40° about the cryostat axis, and the emission was collected at 90° through the appropriate cut-on or interference filters (FWHM ~10 nm) or combinations thereof, with a photodiode (Centronic mod, OSI 5K). The signal was initially detected with a phase sensitive lock-in amplifier (EG&G mod. 5210), digitised and averaged with a computer-controlled LeCroy LT364 oscilloscope triggered by the microwave sweep oscillator.

For absorption-detected measurements (ADMR) the same apparatus was used, but the beam was filtered through a 10 cm water and was focused on a flat cell (1.2 mm path-length) placed perpendicular to the light beam. The transmitted light was analysed by a Jobin–Yvon

HR250 monochromator, equipped with the Data-Link plug-in controlled by a PC, and acquired by the same photodiode used for the fluorescence experiments. The signal is presented as the ratio of the amplitude modulated and the continuous components ($\Delta I/I$) of the photodiode signal corresponding to $\Delta A/A$ for small changes in transmission that are generally not larger than 10^{-5}.

Deconvolution analysis of FDMR/ADMR spectra. Deconvolution analysis in terms of Gaussian sub-bands of the fluorescence emission spectra was performed using a global convolution routine, employing a laboratory-developed software, as previously described (Santabarbara et al. 2002a, 2015; Santabarbara and Carbonera 2005). In brief, the |D|+|E| and |D|-|E| resonance lines of the FDMR spectra, recorded at multiple emission wavelengths, were simultaneously fitted using a linear combination of Gaussians as the model function. The microwave frequency of the Gaussian maxima and bandwidths were considered as global fit parameters and then constrained to assume the same value for the different spectral series (|D|+|E| or |D|-|E|). The amplitudes were instead treated as local parameters and hence allowed to change at the different emission wavelengths. Yet the ratio of the amplitudes, and of the widths of the Gaussian bands, in the |D|+|E| and |D|-|E| transitions were constrained to be the same. To take into account the differences in the signal to noise levels between the microwave spectra recorded at different emission wavelengths, the root mean square noise over the average signal in microwave regions that did not induce triplet sublevel resonance (off-resonance), served as an estimator of data point uncertainties. The search for the best fit parameters was performed with a non-linear least-square algorithm which minimises the global (sum over all measured transitions) χ^2 likelihood indicator, performing an initial search through the Simplex algorithm and a refinement using a Levenberg-Marquard algorithm (Santabarbara et al. 2007, 2015).

Time-resolved electron magnetic resonance. TR-EPR experiments were performed on a Bruker ELEXSYS E580 spectrometer operating at X-band (9.66 GHz), equipped with a dielectric cavity (Bruker ER 4117-DI5, TE_{011} mode), an Oxford CF935 liquid helium flow cryostat and an Oxford ITC4 temperature controller. The microwave frequency was measured by a frequency counter (HP5342A). The temperature was controlled by an helium flow system, disabling the magnetic field modulation and using pulsed sample photo-excitation from a Nd:YAG pulsed laser (Quantel Brilliant) equipped with both second and third harmonic modules and an optical parametric oscillator (OPOTECH) (λ = 472 nm, pulse length = 5 ns, E/pulse $\cong$ 3 mJ, 10 Hz repetition time). The experiments were carried out by recording the time evolution of

the EPR signal after the laser pulse with a LeCroy 9360 digital oscilloscope triggered by the laser pulse. At each magnetic field position, 80 transient signals were usually averaged before transferring them to the PC controlling the instrument via the XEPR software; 250 points on the magnetic field axis were recorded, with a sweep width of 100.0 mT. The microwave power for TR-EPR experiments was set to 0.47 mW (25 dB attenuation). The time vs. field surfaces were processed using a home-written MATLAB program that removes the background signal before the laser pulse (signal vs. magnetic field) and the intrinsic response of the cavity to the laser pulse at an off-resonance field (signal vs. time). The TR-EPR spectra shown in the main text were extracted from the surfaces at the maximum of the transient (1500 ns after the laser flash) to avoid potential distortions arising from anisotropic relaxations.

Analysis of the TR-EPR spectra and their simulations were performed using Easyspin, a MATLAB toolbox (Stoll and Schweiger 2006).

Results.

Fluorescence Detected Magnetic Resonance of Chl triplet states. The photo-induced triplet states in thylakoid membranes of *A. marina* were initially investigated by FDMR employing broadband detection through a cut-on filter with half transmission at 715 nm. This corresponds, at the measurement temperature of 1.8 K, to integrating over almost the entire emission bandwidth. Thylakoids were at first studied in dark adapted and redox ambient conditions (Figure 1), and employing amplitude modulation settings (33.3 Hz) optimised for lifetimes of ~1-3 ms, as expected for unquenched Chl triplet states (Krasnovsky 1982). The presence of more than a single triplet population was observed both in the 510 – 670 MHz (|D|-|E|) and 810 – 970 MHz (|D|+|E|) transitions. Based on the previous analysis of Chls *a* and *d* in organic solvents (Di Valentin et al. 2007), the resonance frequency between 510 – 670 MHz is assigned to Chl *d* |D|-|E| transitions, whereas the Chl *d* |D|+|E| transition is more overlapped to that of Chl *a*, and hence less diagnostic. The |D|-|E| transition of Chl *a* is expected to fall in the 680 – 820 MHz window instead, where it was not possible to detect any signal under the conditions employed (Figure S1). This could be in part due to the fluorescence being substantially dominated by Chl *d* emission; yet Chl *a* triplet states could still be observed on Chl *d* emission because of singlet-singlet energy transfer, as observed for excited state coupling with

long wavelength emitting forms in other photosynthetic complexes **(**e.g. (Searle et al. 1981; Searle and Schaafsma 1992; Carbonera et al. 1997; Santabarbara et al. 2002a)).

Previous ODMR investigations of triplet states in thylakoids of organisms in which Chl *a* is the dominant chromophore involved in photochemical reactions under non-reducing conditions, showed the presence of a Chl *a* triplet population having an unusually short lifetime in the μs time scale (Santabarbara et al. 2002a). Similarly fast-relaxing Chl *a* triplet states were also observed in isolated PSII either by transient spectroscopy (Hillmann et al. 1995; van Mieghem et al. 1995) or TR-EPR (Feikema et al. 2005). In ODMR investigations, this triplet state became dominant under phase sensitive detection at higher amplitude modulation frequencies of the resonant field (333 Hz) than those employed for ms-lifetime populations (Santabarbara et al. 2002a, 2003). Measurements performed under these conditions, however, did not reveal either the presence of additional populations that might emerge because of phase-suppression, or any enhancement and/or changes in the FDMR spectral profile (Figure S1) indicating that the triplets observed under non-reducing conditions are all characterised by the typical lifetime of a few milliseconds.

The population of Chl triplet states is typically favoured under reducing conditions that lead to the accumulation of electron equivalents at the photosystems acceptor side, particularly the accumulation of the fully reduced form of the quinones, namely Q_A in PSII and A_1 in PSI. Under such conditions, the singlet radical pair becomes long-lived since electron transfer to the next acceptor in the chain is prevented, thereby promoting spin dephasing to the triplet state (Budil and Thurnauer 1991). The triplet in the RC can then be populated with high yield by the recombination mechanism.

An efficient method to obtain a complete reduction of the quinone acceptor is that of illuminating the sample in the presence of reducing agents, such as sodium dithionite (Carbonera et al. 1994, 1997; Santabarbara et al. 2002a, 2007), or to expose the samples to long incubation in the dark in the presence of reducing agents (Frank et al. 1979; Gast et al. 1983; Rutherford and Sétif 1990). Yet, upon incubation of *A. marina* thylakoids in the presence of dithionite (in concentration of 1-40 mM, and pH 7-10) a very rapid change in colour of the suspension was observed, which was also accompanied by the pronounced bleaching of Chl absorption (Figure S2). Although the origin of the degradation is not clear at present, it may relate to some non

specific redox reactivity between Chl *d* and dithionite that makes the conditions promoting the population of RC triplets in Chl *a*-binding photosystems not readily transferrable to *A. marina*.

In an attempt to overcome this limitation, the quinone photo-accumulation treatment was performed with a milder reducing agent, sodium ascorbate (Asc, 10-40 mM), alone or in the presence of the redox mediator N,N,N',N'-tetramethyl-para-phenylene-diamine (TMPD, 80 μM). Based on the redox properties of Chl *a*-binding RCs, these sets of conditions shall be sufficient to elicit at least a substantial accumulation of fully reduced Q_A in PSII (Diner and Rappaport 2002 and references therein), but shall not be efficient in promoting the full reduction of A_1 in PSI since the acceptor side of PSI operates at much more negative redox potentials than that of PSII (Brettel 1997 and references therein). Moreover, Asc can also act as an electron acceptor, thereby releasing reducing equivalent accumulation at PSI acceptor side (Trubitsin et al. 2014)

Although illumination in the presence of 10 mM Asc alone was sufficient to induce a significant extent of recombination triplet in a PSII preparation isolated from land plants (Figure S3), the reducing agent alone, even at higher concentrations, did not appear to change by any significant extent the FDMR signals, neither in terms of band-shape or intensity, in the thylakoids of *A. marina* (Figure 1). A significant change in the relative intensity of the different subpopulations was obtained upon illumination in the presence of Asc and TMPD acting as a redox mediator. In particular, there was a strong decrease in the signal of the triplets having a positive amplitude (under the phase convention used in the measurements) and a marked increase in signal intensity in triplets having a negative amplitude. Thus, FDMR spectra obtained in non-reduced/dark adapted membranes and those pre-illuminated in the presence of Asc and TMPD were studied in further detail.

Emission wavelength dependence of FDMR spectra. Figures 2 and 3 show the FDMR spectra recorded at a few selected emission wavelengths using interferential filters (FWHM ~10 nm). Also shown in the figures is the Gaussian sub-bands decomposition of the FDMR spectra by a constrained global fitting approach (described in Material and Methods) in which the spectra acquired in the two different conditions discussed above are simultaneously fitted. This approach allowed the identification of a total of four triplet populations, characterised by the centre frequency, bandwidth, and associated zfs parameters reported in Table 1. The relative abundances of these populations were found to largely depend on the treatments performed at RT

before freezing. In dark-adapted thylakoids under non reducing conditions (Figure 2), three triplets were mainly observed (labelled as a T_1, T_2 and T_3, zfs: |D|: 0.0252 cm^{-1}, |E|: 0.0049 cm^{-1}; |D|: 0.0245 cm^{-1}, |E|: 0.0049 cm^{-1}; |D|: 0.0245 cm^{-1}, |E|: 0.0042 cm^{-1}, respectively), with the first two having almost equal amplitude and being overall the most represented at all the emission wavelengths investigated, whereas the T_4 population was fundamentally negligible. In thylakoids illuminated at RT in the presence of Asc and TMPD the T_3 (|D|: 0.0245 cm^{-1}, |E|: 0.0042 cm^{-1}) and T_4 (|D|: 0.0248 cm^{-1}, |E|: 0.0040 cm^{-1}) populations became the most represented instead, particularly T_3 being the dominant one, whereas both T_1 and T_2 undergo an evident decrease in amplitude, with the latter being almost completely suppressed (Figure 3).

The significant increase of the T_3 and T_4 populations under conditions expected to lead to the accumulation of reducing equivalents, at least at the PSII donor side, would seem to suggest that these Chl *d* triplets are associated with RC processes. It is yet worth nothing that the observed increase in the intensity of FDMR signals associated with T_3 (and T_4) under reducing conditions, although significant, is far less pronounced than that previously reported for Chl *a*-binding photosystems, either isolated (Carbonera et al. 1997) or embedded in the thylakoid membranes (Carbonera et al. 1997; Santabarbara et al. 2002a, 2003, 2007), albeit observed under stronger reducing conditions. This may be due to an only partial reduction of the photosystems' acceptors. The poising conditions employed are expected to efficiently reduce the PSII acceptor, but not to be very effective on PSI terminal acceptors, as they operate at much more negative potential values (< – 500 mV). Hence, to gain further insight into the nature of the triplet populations which displayed the largest sensitivity to the redox/illumination pre-treatment, the samples were also investigated by absorption detected magnetic resonance.

Absorption Detected Magnetic Resonance of Chl d Triplets. Figure 4 shows the ADMR spectra recorded in the |D|-|E| transition in *A. marina* thylakoids pre-illuminated at RT in the presence of Asc and TMPD, at selected wavelengths in the Q_y transition. Also shown in Figure 4 is the decomposition in Gaussian sub-bands, which demonstrates that the ADMR signal was almost entirely due to the two already discussed populations T_3 and T_4, with the former being the dominating species and T_4 accounting on average for ~15-25% of the overall ADMR signal depending on the detection wavelength.

Further details can be gained by recording the Triplet-minus-Singlet (TmS) spectrum. Figure 5 shows the TmS spectra obtained upon microwave excitation in the |D|-|E| transition at

610 MHz. The spectrum displays a broad and asymmetric maximal singlet bleaching centred at about 740 nm, accompanied by a complex set of satellite bands, the most clearly resolved being two sharp derivative-like features having maximal bleaching at 732 nm and 722 nm and positive companion bands at 728 and 717 nm, respectively. Other side bands are observed at 708 and 697 nm.

The TmS spectrum in Figure 5 has some significant similarities with the one recorded in highly PSI enriched particles from *A. marina* by transient optical spectroscopy at 5 K (Schenderlein et al. 2008). This signal became detectable upon pre-illumination of the sample at 230 K in the presence of dithionite and phenazine methosulfate (PMS) as a mediator and was attributed to the PSI RC triplet, $^3P_{740}$. However, the TmS spectrum recoded here by ODMR in thylakoids at 1.8 K shows some additional spectral features. In particular, the sharp bleaching at 732 was not resolved in the previously reported spectrum and the exact position of the satellite bands, with the positive one at ~725 nm and also the side bands at ~705 nm, appearing more defined in the mw-induced TmS. The transient optical TmS showed a bleaching at ~685 nm, which is, however, not resolved here in the mw-induced one (Figure 5).

According to the decomposition of the ADMR spectra (Figure 4), at the pump mw used to record the TmS spectrum (610 MHz) the T_3 ($|D|=0.0245$ cm^{-1}, $|E|=0.0042$ cm^{-1}) population should be by far the dominant one. Hence, although it is possible that some of the fine spectral structure may be the result of partial excitation of the T_4 population, this will require the TmS associated to each of these two states to be significantly different. The relative contribution of the T_3 and T_4 in ODMR spectra at different wavelengths appears to be almost the same (Figures 3 and 4) instead. It has not been possible, however, to record a TmS spectrum with preferential excitation of T_4 (mw > ~630 MHz) because of the signal weakness. Nonetheless, it appears unlikely, albeit not impossible, that the additional features in the $^3P_{740}$ TmS spectrum observed by ODMR with respect to the transient optical methods stem from lack of selective excitation, especially considering that optical excitation does not allow for triplet population selections, unless the populations have sufficiently different lifetimes.

The two dominating triplets, T_3 and T_4, observed after pre-illumination of *A. marina* thylakoids under mildly reducing conditions, most probably represent two sub-populations of a triplet state located on the same chromophore, with the subtle variation in zfs and triplet sub-level resonance frequency resulting from microscopic heterogeneity in the protein-cofactor

coordination. Similar heterogeneities have been previously observed in ODMR investigations of $^3P_{700}$ in Chl *a*-binding PSI, in both isolated photosystems (Carbonera et al. 1997) and more intact environments (Santabarbara et al. 2002a, 2007).

In Figure 5, a decomposition of the TmS spectrum is also shown, with the fit parameters reported in Table 2. According to the Gaussian decomposition the main singlet bleaching bands are centred at 740 nm, 731 nm and 722 nm. As readily visible directly from the TmS spectrum inspection, the bleaching bands at 731 nm and 722 nm are relatively narrow (FWHM 4-4.5 nm), whereas the 740 nm is fairly broad (FWHM ~30 nm). The positive companion bands appear relatively narrow (3.5 – 7 nm, Table 2) as well. The obtained sub-bands shall reflect the shift and population redistribution of the singlet exciton (eigen)states upon population of the RC triplet state. Yet, the exact positions derived from fitting are subjected to some uncertainties, because of cross-compensation of positive/negative amplitude sub-bands, therefore, the description shall be considered as a first-order approximation only (an alternative solution is presented in the Supplementary Information, with slightly different band centres and widths, but displaying an overall consistency, Figure S4).

The broadness of the red-most transition, typically centred at 700-705 nm, is a characteristic also of Chl *a*-binding PSI (Carbonera et al. 1997). Although the exact bleaching positions and band widths are in part species dependent (Witt et al. 2003; Nakamura et al. 2011), the width is most likely affected by a large contribution from homogenous broadening that depends on the electron-phonon coupling, rather than an unusually large heterogeneous broadening (site distribution). The large homogeneous broadening can in principle be due to coupling with a higher (mean) frequency mode with respect to Chls showing a narrow bleaching, to a larger Hung-Rhys, *S*, factor or both (e.g. (Gillie et al. 1989; Jankowiak and Small 1993; Jankowiak et al. 2011). For Chl *a*-binding PSI a large value of *S* (~2-4) was suggested to result from the mixing with a charge-transfer state (Lathrop and Friesner 1994; Renger and Schlodder 2006) that in turn might be favouring a radical pair formation. If this were the case, the broadness of the main bleaching band at 740 nm in the PSI of *A. marina* seems to suggest a conservation of the partial charge-transfer character, as the main bleaching appears to be as broad, or broader, than in standard PSI.

Time-resolved electron paramagnetic resonance. TR-EPR experiments were performed to further characterise the mechanism of triplet population in the thylakoids of *A. marina*. The

two conditions in which the membranes were either dark adapted at ambient conditions or pre-illuminated at RT in the presence of Asc and TMPD were tested by recording the TR-EPR spectra at 50 K, upon laser excitation at 472 nm. Similar results were obtained also performing the measurements at 10 and 100 K (not shown).

Figure 6 shows the TR-EPR spectra obtained in the two investigated conditions. In both spectra, a narrow signal was observed in the centre of the spectrum (g ~ 2.00, magnetic field ~ 344 mT), that can be attributed to spin correlated radical pairs. Its characterization is beyond the scope of the present investigation.

Under non reducing conditions, the TR-EPR spectrum was dominated by a triplet state contribution characterised by the polarisation pattern expected for a triplet state populated by the ISC mechanism (*eaeaea*), which would then be most likely populated in the photosystems' antenna. This triplet population(s) shall correspond, mainly, to the T_1 and T_2 retrieved by ODMR (Figure 2, Table 1), also noticing that T_3 was already detectable under these conditions. However, the polarisation pattern of the triplet states observed in the membrane illuminated under mildly reducing conditions was still *eaeeaea* meaning that, also in this case, the triplets become populated by the ISC mechanism. On the contrary, the recombination mechanism should lead to an *aeeaae* pattern (see Figure 6). This is a surprising result, since the conditions used should promote the recombination-induced RC triplet population. ODMR clearly detected a redistribution of the triplet populations after the pre-illumination treatment, with T_3 becoming the dominant one, followed by T_4 (Figure 2, Table 2), therefore, these are most likely the triplets also observed by TR-EPR. Yet, the treatments were not accompanied by a change in the population mechanism of the triplet states. The zfs parameters determined from the EPR spectra are compatible with those derived from the FDMR deconvolution (Table 2), but unfortunately, the intrinsically lower zfs resolution of EPR and the difference in temperature do not allow to discern between the four components identified in the FDMR datasets. It is worth mentioning that a suppression of the recombination triplet signal like the one previously reported for the heliobacterial reaction centre, in which the recombination triplet ($^3P_{800}$) was not spin polarised because of the D/E ratio being close to 3, with consequent cancellation of the absorptive and emissive contributions to the spectrum (Ferlez et al. 2017), can be excluded on the basis of the D and E values determined in ODMR (see Table 1), that are characterised by a D/E ratio between 5 and 6 in all cases.

Discussion

The investigation of photo-induced chlorophyll triplet states in the isolated thylakoid membranes of *A. marina* revealed some interesting peculiarity of the mechanisms of population of these excited states in Chl *d*/*a* binding photosystems. The characterization remains, for the time being, limited by the difficulties in employing the reducing conditions commonly used for Chl *a*-binding photosystems. This is due to the rapid degradation of the *A. marina* photosystems, manifesting as a strong, non specific, absorption bleaching accompanied by an obvious change in colour of the thylakoid suspension and loss of both detectable ODMR and EPR signals. Hence, the investigation was restricted to the use of mildly reducing conditions, accompanied by illumination at room temperature.

Photo-induced triplet states in A. marina thylakoids under non reducing and moderately reducing conditions: absence of signal attributable to ^{3}Chl a or ^{3}PSII-RC

Under none of the conditions investigated in this study it was possible to observe photo-induced Chl *a* triplet states. Instead, all the ODMR and TR-EPR triplet signals were assigned to Chl *d*, based on their zfs parameters and resonance frequencies (Figures 1-3 and 7, Table 1).

In Chl *a*-binding PSII RC a fast-decaying (microsecond) triplet state was reported to be populated (Santabarbara et al. 2002a, 2003) even under non-reducing conditions and was assigned to the recombination triplet state. The decrease of the triplet state lifetime under these conditions was suggested to be due to the presence of a so-called "observer spin" (or radical) on Q_A^- in proximity of the Chl *a* cluster composing the RC (Hillmann et al. 1995; van Mieghem et al. 1995). Yet, in *A. marina* thylakoids it was not possible to detect any, neither Chl *a* nor *d*, fast decaying triplet. Together with the detection of long-lived ^{3}Chl *d* only, this observation might be taken as a favourable evidence for Chl *d*, rather than Chl *a*, being the main, or even the only, photoactive pigment both in PSI and PSII of this organism. However, the absence of any significant long-lived ^{3}Chl *a/d* attributable to the PSII RC after illumination under mildly reducing conditions is puzzling. This treatment was tested and proved to be efficient in promoting recombination triplet population in canonical Chl *a*-binding PSII (Figure S3) and was then expected to be effective also in *A. marina* since the redox properties of its PSII acceptor side were shown to be almost the same as those of canonical PSII (Cser and Vass 2007; Cser et al. 2008; Viola et al. 2022). Moreover, the reported shift of ~ 60 mV in the redox potential of Pheo

a in *A. marina* PSII should lead to a decrease in the energy gap with Q_A and hence potentially favour, with respect to canonical Chl *a* PSII, the repopulation of the [P^+Pheo^-] radical pair that, being the precursor for ^{3}PSII-RC, is expected to increase the overall triplet yield in the Chl *d*-dominated RC. A higher triplet population was proposed as the cause of the increased sensitivity to light-induced damage and propensity in $^1O_2$ production in this organism with respect to Chl *a*- and Chl *a*/*f*-binding PSII (Viola et al. 2022). The results obtained here in thylakoids do not appear, however, to indicate a higher yield of ^{3}PSII-RC in *A. marina*. It is possible that the increased sensitivity to damage and the proposed higher PSII-RC triplet population, might be observable at RT but not at the cryogenic temperatures employed in ODMR (1.8 K) or TR-EPR (10–100 K). It is worth noting that these are however necessary conditions to observe ^{3}PSII-RC by EPR methods, that in Chl *a*-binding RCs are typically in excellent correlation with optical measurements that can be performed also at physiological or close-to-physiological conditions.

Although it is not possible, at present, to unambiguously determine the reasons leading to ^{3}Chl in PSII of *A. marina* escaping detection, it is nonetheless possible to advance some hypothesis. One possibility is that the PSII acceptor side in thylakoids is, to some extent, only partially accessible to the redox reagents and mediators; this, in turn, will make the pre-treatment employed in this study inefficient. Another possibility, which is, however, not very likely especially at 1.8 K where ODMR experiments are performed, is that the triplet might be populated but escapes detection due to unusually fast spin-lattice relaxation. Finally, it may be considered the hypothesis that the recombination triplet is not efficiently populated because the other de-excitation routes of the precursor radical pair, such as recombination to either the excited or the ground state, dominate in the PSII of this organism.

Studies on PSII of *A. marina* on the isolated, purified, supercomplex will be necessary to interpret the absence of ^{3}RC formation even under conditions that should, in principle, promote it.

Photo-induced ^{3}Chl d triplet states in A. marina thylakoids under non reducing and moderately reducing conditions are dominated by PSI-bound chromophores

The combination of FDMR and ADMR analyses, in particular the TmS spectrum recorded upon mw excitation at 610 MHz (|D|-|E|), seems to indicate that, at least under moderate reducing conditions, the detected ^{3}Chl *d* states (populations T_3 and T_4) in *A. marina* thylakoids belong to PSI chromophores. The assignment is based on specific spectral features,

like the maximum broad bleaching at 740 nm, and the intense flanking bands at ~730 and ~720 nm, being shared by the mw-induced TmS spectrum (Figure 5) and the spectrum previously obtained by transient optical spectroscopy in highly enriched PSI particles (Schenderlein et al. 2008). The sensitivity to illumination under mild reducing conditions and the complex spectral shape would suggest that T_3 (and likely also T_4 that might be only a subtly different conformer) sits on a Chl *d* that is part of PSI RC. However, differently from what may be expected in view of the response to the (mild) redox poise, this triplet state does not show the characteristic *aeeaae* polarisation pattern resulting from the almost pure population of the T_0 level when the triplet stems from a singlet radical pair state precursor, that is by the recombination mechanism. It rather displays the *eaeaea* polarisation pattern that is instead compatible with the ISC mechanism (Di Valentin et al. 2007). This is actually the same electron spin polarisation observed under non-reducing conditions (Figure 6) when the dominating triplets (T_1 and T_2) are most likely populated in the antenna.

The triplet assigned to PSI-RC (T_3) is already detected, although not being the dominant species, under non reducing conditions (Figure 2). This is similar to what previously reported for both isolated Chl *a*-binding PSI (Carbonera et al. 1997) and thylakoids embedded PSI (Santabarbara et al. 2002a, 2007) that, moreover, also showed a heterogeneity of resonance transitions, distinguishable by FDMR because of the very high sensitivity of the technique to even very subtle variations in the zfs parameters.

The significant damping of the populations T_1 and T_2 under the mildly reducing conditions employed, that correlates with the increase of populations T_3 and T_4, suggests that they originate from the same photosystem, being in competition for localisation of the singlet excited state on the Chl *d* molecule(s) from which the triplet is then formed. Similar behaviours have been previously observed in Chl *a*-binding PSI (McLean and Sauer 1982; Carbonera et al. 1997). However, it shall be noted that the fluorescence emission spectra of PSI and PSII of *A. marina* are not quite as distinguished as those of Chl *a*-binding super-complexes, where PSI shows a red-shift of at least 20 nm, and commonly as large as 30-40 nm, with respect to PSII in most model organisms (e.g. for reviews Croce and van Amerongen 2013; Santabarbara et al. 2020). In this respect, the emission wavelength selectivity offered by FDMR is less unambiguous for the Chl *d/(a)*-binding photosystem. Although it is, therefore, not possible to exclude completely that one of the T_1 and T_2 population, or both, might stem, at least in part, from PSII

antenna, the observed decrease in population after illumination under mildly reducing conditions indicates a dominance of PSI-bound chromophores to these triplet populations.

Triplet states in Chl d-binding PSI RC of A. marina: an alternative population mechanism?

The surprising observation that the ^{3}Chl *d* population that increases upon illumination under mildly reducing conditions, namely T_3, shows a TmS spectrum that closely resembles the one previously reported and assigned to PSI-RC (Schenderlein et al. 2008), $^3P_{740}$, but manifests an electron spin polarisation resulting from ISC, deserves further attention and discussion.

One hypothesis to reconcile this apparently contradicting evidence is that the observed bleaching in the TmS spectrum at 740 nm does not correspond to the same molecule, or cluster of excitonically coupled molecules, giving rise to the bleaching at 735-740 nm upon light-induced cation formation (P_{740}^+). The TmS and the P^+-minus-P spectra are not expected to be exactly the same because, whereas ^{3}P is electrically neutral and the spectral feature shall originate from excitonic interaction only, the charged nature of P^+ (and often the concomitant presence of a reduced acceptors, A^-) gives rise to local electric field manifesting a Stark effect (also called electrochromic) on pigments that also contribute to the difference spectrum. Thus, the differences in fine structure of the previously reported P^+-minus-P and ^{3}P-minus-P spectra (Schenderlein et al. 2008), with the main bleaching being located almost at identical positions, might just be due to the contribution from local Stark band-shifts. It can not however be completely excluded, instead, that the triplet sits on a different (cluster of) chromophore, having the lowest singlet state at almost the same energy as P_{740}. This would, in other terms, represent a low-energy Chl *d* spectral form (red form) in *A. marina* PSI antenna, being almost iso-energetic with the lowest RC excited state. Red forms are characteristics of many Chl *a*-binding PSI (Croce and van Amerongen 2013; Santabarbara et al. 2020). Their presence has been reported in the isolated PSI of *A. marina* both by low temperature optical spectroscopy and the associated structure-based spectral-kinetic modelling (Kimura et al. 2022). On the other hand, the response of the T_3 population to illumination in the presence of mediators does not corroborate this hypothesis, because the lowest energy state shall remain, at low temperature, a (local) singlet exciton trap irrespectively of the reduction state of the photosystem acceptor side.

The second hypothesis, that we tend to favour, is that the T_3 population does actually represent a triplet sitting on one of the Chl *d* present in the PSI RC, but being populated with a

different mechanism than in Chl *a*-binding PSI, *i.e.* not through the recombination mechanism. The recombination mechanism can be expressed, in simplified kinetic terms, by the following generalised scheme:

$$RC^{*} \xrightarrow[\longleftarrow]{k_{css}} \left(\begin{array}{l} {}^{1}[P^{+}A^{-}] \xleftrightarrow[\omega]{} \left(\begin{array}{l} {}^{3}[P^{+}A^{-}] \\ \downarrow \\ {}^{3}P \end{array} \right) \end{array} \right) \qquad \text{Scheme 1}$$

Where ${}^{3}[P^{+}A^{-}]$ and ${}^{1}[P^{+}A^{-}]$ are the triplet and singlet state of the spin-correlated radical pair, respectively, formed with an effective rate constant k_{css} from the reaction centre excited state RC^{*}. ω is the singlet-triplet mixing frequency of the radical pair, and the triplet becomes finally localised on ${}^{3}P$, with P being one (or more) of the chromophores composing the RC, having the lowest triplet energy. This mechanism is kinetically favoured when ω is much faster than the rate of direct recombination from ${}^{1}[P^{+}A^{-}]$ to the reaction centre excited state RC^{*}, which is shown, but unlabelled, in scheme 1, to stress that it represents a "slow" kinetic process.

If the recombination rate to the singlet state (k_{sr}) becomes significant or even dominant, the kinetic scheme can be modified as:

$$\left(\begin{array}{l} RC^{*} \underset{k_{sr}}{\overset{k_{css}}{\rightleftarrows}} {}^{1}[P^{+}A^{-}] \\ \downarrow \\ {}^{3}P \end{array} \right) \xleftrightarrow[\omega]{} {}^{3}[P^{+}A^{-}] \qquad \text{Scheme 2}$$

In this case, repopulation of RC^{*} would kinetically out-compete the population of the radical pair triplet state. Then, under this scenario, the triplet would be populated by ISC, analogously to the mechanism observed for Chl molecules in the antenna.

An increase in the rate of RC singlet state repopulation can be caused by a relatively small free energy difference, making the population of the radical pair rapidly reversible. Photochemical mechanisms involving a substantial equilibration between the primary radical

pair and the reaction centre (or antenna bed) excited state have been extensively discussed, for instance by Holtzwart and cowokers (Schatz et al. 1988), initially in Chl *a*-binding PSII and have been successively extended to PSI (Müller et al. 2003, 2010). Yet, following primary photochemistry, the charge separated state was discussed as being stabilised through the almost irreversible formation of a secondary radical pair, either by electron or hole transfer. Recombination to the triplet state in the RC takes place from the latter "stabilised", and hence relatively long lived, radical pair. In Chl *a*-binding PSI this state corresponds to $[P_{700}^{+}A_{0}^{-}]$, where A_0 is the Chl *a* at the structural eC_3 position, acting as the electron acceptor. The proposed RC triplet population in the PSI of *A. marina* by ISC would require that the energy gap between RC^{*} and the corresponding radical pair to be much smaller than in canonical PSI, particularly considering that at ODMR measurement condition of 1.8 K the thermal energy for uphill transfer is only 0.15 meV, and hence the radical pair to be almost iso-energetic with RC excited state.

A decrease in the driving force for primary photochemistry and successive charge stabilisation reactions might be expected considering the lower photon energy of P_{740}^{*} with respect to P_{700}^{*}, which is in the order of ~95-100 meV. On the other hand, the structural model of *A. marina* PSI showed the presence of Pheo *a* at the eC_3 position. The triplet precursor radical pair in *A. marina* PSI should then be $[P_{740}^{+}Pheo^{-}]$. The reduction midpoint potential of Pheo *a* in organic solvents is 100-200 mV more positive than that of Chl *a* (Kobayashi et al. 2013), which in principle can even over-compensate the photon energy loss in P_{740}^{*}. Hence, for the proposed mechanism for PSI-RC triplet proceeding through ISC to hold true, and the energy gap between RC^{*} and $[P_{740}^{+}Pheo^{-}]$ to be particularly small, the potential of Pheo *a* at the eC_3 site shall be tuned by the photosystem subunits to significantly more reducing values than expected based on the comparisons with Chl *a* in organic solvents. A small energy gap cannot instead be ascribed to differences in the oxidation potential of P_{740}^{+} and P_{700}^{+}, that differ only by about 10 mV as estimated by direct titration (Schenderlein et al. 2008).

It shall also be worth considering that, most studies that discussed a reversible radical pair mechanism in canonical PSI, postulated the population of a primary radical pair, acting as precursor to $[P_{700}^{+}A_{0}^{-}]$ (Müller et al. 2003, 2010; Holzwarth et al 2005; Giera et al. 2010, Molotokaite et al. 2017; Russo et al. 2020). The energy gap in between RC^{*} and the primary

radical pair, comprising the cofactors at the eC_2 position is therefore smaller than between the further stabilised pair. Thus, the decrease in the driving force for the primary charge separation could favour in *A. marina* recombination to RC^* starting from the primary charge separated state rather than from the secondary $[P_{740}^+ Pheo^-]$.

Although the proposed mechanism provides a rationale for the observation of the *eaeaea* instead of the *aeeaae* polarisation pattern for a triplet state residing on the RC, it remains to be validated by experimental approaches through which the free energy difference between RC^* and $[P_{740}^+ Pheo^-]$ could be assessed (*i.e.* ultrafast transient absorption, delayed luminescence).

Conclusions

The investigation of triplet states by ODMR and TR-EPR in the thylakoid membranes of *A. marina* allowed to identify the presence of four different triplet populations, which can all be assigned to Chl *d* based on their microwave resonance frequencies and associated zfs parameters. All ^{3}Chl *d* populations appear to be long-lived, having a ms-lifetime. On the other hand, neither short- or long-lived Chl *a* triplet states could be detected under the conditions employed.

The ^{3}Chl *d* populations display different behaviour in response to the treatment in the presence of mild redox poise and pre-illumination at RT. In particular, a population characterised by zfs $|D|=0.0245$ cm^{-1} and $|E|=0.0042$ cm^{-1} increases and becomes dominant following sample illumination in the presence of a weak reductant. Its associated TmS spectrum, detected at a resonant frequency of 610 MHz at 1.8 K, resembles the one previously attributed to $^3P_{740}$, the PSI reaction centre triplet, by optical spectroscopy at 5 K (Schenderlein et al. 2008). Moreover, the microwave-induced TmS spectrum presents additional fine spectral features. Surprisingly, TR-EPR spectroscopy indicates that this triplet is populated through ISC rather than the recombination mechanism. A possible explanation for this apparent contradiction is proposed, based on kinetic competition between the singlet-triplet mixing and the repopulation of the RC singlet excited state, from the precursor radical pair $[P_{740}^+ Pheo^-]$. Population of $^3P_{740}$ by ISC can become efficient if recombination to RC^* is the dominant kinetic process. This would in turn imply a significantly lower energy gap between RC^* and the precursor radical pair state than in canonical, Chl *a*-binding, PSI.

Acknowledgments

SS and APC acknowledge support from Regione Lombardia through the project "Enhancing Photosynthesis" (DSS 16652 30/11/2021) on behalf of the winners of the "Lombardia è Ricerca – 2020" award. AAP acknowledge support from by Russian Science Foundation Grant RSF 21-74-10085. AA and DC acknowledge financial support from the University of Padova (P-DiSC-2019). MB acknowledges support from P-DiSC#02BIRD2020-UNIPD.

Figure Legends

Figure 1. FDMR spectra of *A. marina* thylakoids recorded through a long-pass filter (λ>715 nm) in samples that were **a)** dark adapted for 15 min at RT or illuminated for 5 minutes at RT following incubation with **b)** 10 mM Asc **c)** 40 mM Asc **d)** 10 mM Asc and 80 μM TMPD. Measurement conditions: T,1.8 K; mw-amplitude modulation, 33.3 Hz; phase, -96°; scan rate, 2.5 MHz s^{-1}.

Figure 2. Decomposition of FDMR spectra in *A. marina* thylakoids, dark adapted at RT without the addition of reducing agents, at representative emission wavelengths. Black lines: experimental data; red lines: fitted spectra: dash-dotted lines: Gaussian sub-bands, orange (T_1), dark yellow (T_2), green (T_3), blue (T_4). Triplets T_1-T_4 are defined as in Table 1. Measurements conditions as in the legend of Figure 1.

Figure 3. Decomposition of FDMR spectra in *A. marina* thylakoids, illuminated at RT in the presence of Asc (10 mM) and TMPD (80 μM), recorded at representative emission wavelengths. Black lines: experimental data; red lines: fitted spectra: dash-dotted lines: Gaussian sub-bands, orange (T_1), dark yellow (T_2), green (T_3), blue (T_4). Triplets T_1-T_4 are defined as in Table 1. Measurements conditions as in the legend of Figure 1.

Figure 4. Decomposition of ADMR spectra in *A. marina* thylakoids, illuminated at RT in the presence of Asc (10 mM) and TMPD (80 μM), recorded at representative absorption wavelengths in the Chl *d* Q_y band. Black lines: experimental data; red lines: fitted spectra: dash-

dotted lines: Gaussian sub-bands, orange (T_1), dark yellow (T_2), green (T_3), blue (T_4). Triplets T_1-T_4 are defined as in Table 1. Measurements conditions as in the legend of Figure 1, except that the phase was +80 °.

Figure 5. Microwave-induced TmS spectrum obtained upon excitation at 610 MHz, in *A. marina* thylakoids, illuminated at RT in the presence of Asc (10 mM) and TMPD (80 μM). Black lines and open symbols: experimental data; red lines: fitted spectra; dash-dotted lines: Gaussian sub-bands, with green shades representing singlet bleaching and yellow-orange shades describing the increase in absorption upon triplet population; the fit parameters are reported in Table 2. Measurements conditions as in the legend of Figure 1, except that the phase was +80° and the wavelength scan rate was 0.33 nm sec^{-1}.

Figure 6. X-band triplet TR-EPR spectra of *A. marina* thylakoids that were **a)** dark adapted for 15 min at RT or **b)** illuminated at RT in the presence of Asc (10 mM) and TMPD (80 μM). The simulated **c)** ISC and **d)** recombination ^{3}Chl *d* spectra have been calculated using the following parameters: D = 25.8 mT, E = − 5.35 mT, D strain = 2.5 mT, E strain = 1.5 mT, isotropic linewidth = 1.0 mT, microwave frequency 9.649 GHz. For the simulation of the **c)** ISC triplet, a polarisation of (P_x:P_y:P_z) = (0.33:0.43:0.24) has been employed. The spectra have been vertically shifted for a better comparison. *a* = absorption, *e* = emission.

Table 1

Parameters of Gaussian Decomposition of ODMR Spectra of *A. marina* thylakoids						
Triplet	|D|-|E| (MHz)	|D|+|E| (MHz)	FWHM (MHz)	|D| (cm^{-1})	|E| (cm^{-1})	Assignment
T_1	609.7	903.4	22.2	0.0252	0.0049	PSI-Ant
T_2	587.3	883.3	20.8	0.0245	0.0049	PSI(/PSII)-Ant
T_3	608.0	858.4	14.2	0.0245	0.0042	PSI-RC
T_4	622.6	863.5	15.1	0.0248	0.0040	PSI-RC

In Table 1 are reported the values of the maxima and the widths of the Gaussian functions resulting from the global, joint, deconvolution analysis of the FDMR and ADMR spectra recorded in *A. marina* thylakoids dark-adapted under non-reducing and room temperature-illuminated under mild-reducing conditions (10 mM Asc + 80 μm TMPD). Also indicated are the zero field splitting (zfs) parameters |D| and |E|. Errors are in the zfs ±0.0001 cm^{-1}.

Table 2

Gaussian decomposition of mw-induced TmS spectrum in *A. marina* thylakoids			
Band	Centre (nm)	FWHM (nm)	Amplitude
1	644.5	24.7	0.081
2	699.5	15.0	0.382
3	707.9	4.1	0.738
4	717.4	7.2	0.643
5	722.1	4.2	-0.428
6	729.6	3.4	0.950
7	730.9	4.5	-0.784
8	740.1	29.7	-0.692
9	757.4	24.2	-0.067

In Table 2 are reported the parameters employed in the description of the TmS spectrum obtained by microwave excitation at 610 MHz (|D|-|E|) and assigned to a triplet population residing in one or being shared between chromophores composing the PSI reaction centre ($^3P_{740}$) of *A. marina*.

References.

Agostini A, Palm DM, Paulsen H, Carbonera D (2018) Optically Detected Magnetic Resonance of Chlorophyll Triplet States in Water-Soluble Chlorophyll Proteins from Lepidium virginicum: Evidence for Excitonic Interaction among the Four Pigments. J Phys Chem B 122:6156–6163. https://doi.org/10.1021/acs.jpcb.8b01906

Agostini A, Palm DM, Schmitt F-J, et al. (2017) An unusual role for the phytyl chains in the photoprotection of the chlorophylls bound to Water-Soluble Chlorophyll-binding Proteins. Sci Rep 7:7504. https://doi.org/10.1038/s41598-017-07874-6

Akiyama M, Miyashita H, Kise H, Watanabe T, Mimuro M, Miyachi S, Kobayashi M (2002) Quest for minor but key chlorophyll molecules in photosynthetic reaction centers – unusual pigment composition in the reaction centers of the chlorophyll d-dominated cyanobacterium *Acaryochloris marina*. Photosynth Res 74: 97–107. https://doi.org/10.1023/A:1020915506409

Allakhverdiev SI, Kreslavski VD, Zharmukhamedov SK, Voloshin RA, Korol'kova DV, Tomo T, Shen J.R. (2016) Chlorophylls *d* and *f* and their role in primary photosynthetic processes of cyanobacteria. Biochemistry [Moscow] 8:201–212. https://doi.org/10.1134/S0006297916030020

Allakhverdiev SI, Tomo T, Shimada Y, et al. (2010) Redox potential of pheophytin a in photosystem II of two cyanobacteria having the different special pair chlorophylls. Proc Natl Acad Sci 107:3924–3929. https://doi.org/10.1073/pnas.0913460107

Allakhverdiev SI, Tsuchiya T, Watabe K, Kojima A, Los DA, Tomo T, Klimov VV, Mimuro M. (2011) Redox potentials of primary electron acceptor quinone molecule $(Q_A)^-$ and conserved energetics of photosystem II in cyanobacteria with chlorophyll *a* and chlorophyll *d*. Proc Natl Acad Sci U S A. 108:8054-8058. https://doi.org/doi: 10.1073/pnas.1100173108

Bailleul B, Johnson X, Finazzi G, et al. (2008) The Thermodynamics and Kinetics of Electron Transfer between Cytochrome b_6f and Photosystem I in the Chlorophyll d-dominated Cyanobacterium, *Acaryochloris marina*. J Biol Chem 283:25218–25226. https://doi.org/10.1074/jbc.M803047200

Bowers PG, Porter G (1967) Quantum Yields of Triplet Formation in Solutions of Chlorophyll. Proc R Soc Lond A Math Phys Sci 296:435–441

Brettel K (1997) Electron transfer and arrangement of the redox cofactors in photosystem I.

Biochim Biophys Acta - Bioenerg 1318:322–373. https://doi.org/10.1016/S0005-2728(96)00112-0

Budil DE, Thurnauer MC (1991) The chlorophyll triplet state as a probe of structure and function in photosynthesis. Biochim Biophys Acta - Bioenerg 1057:1–41. https://doi.org/10.1016/S0005-2728(05)80081-7

Carbonera D (2009) Optically detected magnetic resonance (ODMR) of photoexcited triplet states. Photosynth Res 102:403–414. https://doi.org/10.1007/s11120-009-9407-5

Carbonera D, Collareta P, Giacometti G (1997) The P700 triplet state in an intact environment detected by ODMR. A well resolved triplet minus singlet spectrum. Biochim Biophys Acta - Bioenerg 1322:115–128. https://doi.org/10.1016/S0005-2728(97)00068-6

Carbonera D, Giacometti G, Agostini G (1992) FDMR of Carotenoid and Chlorophyll triplets in light-harvesting complex LHCII of spinach. Appl Magn Reson 3:859–872. https://doi.org/10.1007/BF03260117

Carbonera D, Giacometti G, Agostini G (1994) A well resolved ODMR triplet minus singlet spectrum of P680 from PSII particles. FEBS Lett 343:200–204. https://doi.org/10.1016/0014-5793(94)80555-5

Cherepanov DA, Shelaev I V., Gostev FE, et al. (2020) Evidence that chlorophyll f functions solely as an antenna pigment in far-red-light photosystem I from *Fischerella thermalis* PCC 7521. Biochim Biophys Acta - Bioenerg 1861:148184. https://doi.org/10.1016/j.bbabio.2020.148184

Croce R, van Amerongen H (2013) Light-harvesting in photosystem I. Photosynth Res 116:153–166. https://doi.org/10.1007/s11120-013-9838-x

Cser K, Deák Z, Telfer A, et al. (2008) Energetics of Photosystem II charge recombination in *Acaryochloris marina* studied by thermoluminescence and flash-induced chlorophyll fluorescence measurements. Photosynth Res 98:131–140. https://doi.org/10.1007/s11120-008-9373-3

Cser K, Vass I (2007) Radiative and non-radiative charge recombination pathways in Photosystem II studied by thermoluminescence and chlorophyll fluorescence in the cyanobacterium *Synechocystis* 6803. Biochim Biophys Acta - Bioenerg 1767:233–243. https://doi.org/10.1016/j.bbabio.2007.01.022

Di Valentin M, Ceola S, Agostini G, et al. (2007) The photo-excited triplet state of chlorophyll d

in methyl-tetrahydrofuran studied by optically detected magnetic resonance and time-resolved EPR. Mol Phys 105:2109–2117. https://doi.org/10.1080/00268970701627797

Diner BA, Rappaport F (2002) Structure, dynamics, and energetics of the primary photochemistry of photosystem II of oxygenic photosynthesis. Annu Rev Plant Biol 53:551–580. https://doi.org/10.1146/annurev.arplant.53.100301.135238

Durrant JR, Giorgi LB, Barber J, et al. (1990) Characterisation of triplet states in isolated Photosystem II reaction centres: Oxygen quenching as a mechanism for photodamage. Biochim Biophys Acta - Bioenerg 1017:167–175. https://doi.org/10.1016/0005-2728(90)90148-W

Feikema WO, Gast P, Klenina IB, Proskuryakov II (2005) EPR characterisation of the triplet state in photosystem II reaction centers with singly reduced primary acceptor QA. Biochim Biophys Acta - Bioenerg 1709:105–112. https://doi.org/10.1016/j.bbabio.2005.07.004

Ferlez B, Agostini A, Carbonera D, et al. (2017) Triplet Charge Recombination in Heliobacterial Reaction Centers Does Not Produce a Spin-Polarized EPR Spectrum. Zeitschrift für Phys Chemie 231:593–607. https://doi.org/10.1515/zpch-2016-0825

Frank HA, McLean MB, Sauer K (1979) Triplet states in photosystem I of spinach chloroplasts and subchloroplast particles. Proc Natl Acad Sci 76:5124–5128. https://doi.org/10.1073/pnas.76.10.5124

Gan F, Zhang S, Rockwell NC, et al. (2014) Extensive remodeling of a cyanobacterial photosynthetic apparatus in far-red light. Science (80-) 345:1312–1317. https://doi.org/10.1126/science.1256963

Gast P, Swarthoff T, Ebskamp FCR, Hoff AJ (1983) Evidence for a new early acceptor in Photosystem I of plants. An ESR investigation of reaction center triplet yield and of the reduced intermediary acceptors. Biochim Biophys Acta - Bioenerg 722:163–175. https://doi.org/10.1016/0005-2728(83)90170-6

Giera W, Ramesh VM, Webber AN, van Stokkum IHM, van Grondelle R, Gibasiewicz K (2010) Effect of the P700 pre-oxidation and point mutations near A0 on the reversibility of the primary charge separation in Photosystem I from *Chlamydomonas reinhardtii*. Biochim. Biophys. Acta 1797: 106–112. https://doi.org/10.1016/j.bbabio.2009.09.006

Gillie JK, Lyle PA, Small GJ, Golbeck JH (1989) Spectral hole burning of the primary electron donor state of Photosystem I. Photosynth Res 22:233–246.

https://doi.org/10.1007/BF00048302

Gobets B, van Grondelle R (2001) Energy transfer and trapping in photosystem I. Biochim Biophys Acta - Bioenerg 1507:80–99. https://doi.org/10.1016/S0005-2728(01)00203-1

Hamaguchi T, Kawakami K, Shinzawa-Itoh K, et al. (2021) Structure of the far-red light utilizing photosystem I of *Acaryochloris marina*. Nat Commun 12:2333. https://doi.org/10.1038/s41467-021-22502-8

Hartzler DA, Niedzwiedzki DM, Bryant DA, et al. (2014) Triplet Excited State Energies and Phosphorescence Spectra of (Bacterio)Chlorophylls. J Phys Chem B 118:7221–7232

Hastings G, Wang R (2008) Vibrational mode frequency calculations of chlorophyll-d for assessing (P_{740}^{+}–P_{740}) FTIR difference spectra obtained using photosystem I particles from *Acaryochloris marina*. Photosynth Res 95:55–62. https://doi.org/10.1007/s11120-007-9228-3

Hillmann B, Brettel K, van Mieghem F, et al. (1995) Charge Recombination Reactions in Photosystem II. 2. Transient Absorbance Difference Spectra and Their Temperature Dependence. Biochemistry 34:4814–4827. https://doi.org/10.1021/bi00014a039

Ho M-Y, Soulier NT, Canniffe DP, et al. (2017) Light regulation of pigment and photosystem biosynthesis in cyanobacteria. Curr Opin Plant Biol 37:24–33. https://doi.org/10.1016/j.pbi.2017.03.006

Holt AS, Morley H V. (1959) A proposed structure for chlorophyll d. Can J Chem 37:507–514. https://doi.org/10.1139/v59-069

Holzwarth AR, Müller MG, Niklas J, Lubitz W(2005) Charge recombination fluorescence in photosystem I reaction centers from *Chlamydomonas reinhardtii*. J. Phys. Chem. B 109:5903–5911. https://doi.org/10.1021/jp046299f

Hu Q, Miyashita H, Iwasaki I, et al. (1998) A photosystem I reaction center driven by chlorophyll d in oxygenic photosynthesis. Proc Natl Acad Sci 95:13319–13323. https://doi.org/10.1073/pnas.95.22.13319

Itoh S, Mino H, Itoh K, et al. (2007) Function of Chlorophyll d in Reaction Centers of Photosystems I and II of the Oxygenic Photosynthesis of *Acaryochloris marina*. Biochemistry 46:12473–12481. https://doi.org/10.1021/bi7008085

Jankowiak R, Reppert M, Zazubovich V, et al. (2011) Site Selective and Single Complex Laser-Based Spectroscopies: A Window on Excited State Electronic Structure, Excitation Energy

Transfer, and Electron–Phonon Coupling of Selected Photosynthetic Complexes. Chem Rev 111:4546–4598. https://doi.org/10.1021/cr100234j

Jankowiak R, Small GJ (1993) Spectral hole burning: a window on excited state electronic structure, heterogeneity, electron-phonon coupling, and transport dynamics of photosynthetic units. In: Deisenhofer J, Norris J (eds) The photosynthetic reaction center, Vol. 2. Academic Press

Kato K, Shinoda T, Nagao R, Akimoto S, Suzuki T, Dohmae N, Chen M, Allakhverdiev SI, Shen JR, Akita F, Miyazaki N, Tomo T (2020) Structural basis for the adaptation and function of chlorophyll *f* in photosystem I. Nat Commun 11:1-10. https://doi.org/10.1038/s41467-019-13898-5

Kaucikas M, Nürnberg D, Dorlhiac G, Rutherford AW, van Thor JJ (2017) Femtosecond visible transient absorption spectroscopy of chlorophyll *f*-containing photosystem I. Biophys. J. 112: 234-249. https://doi.org/10.1016/j.bpj.2016.12.022

Ke B (1973) The primary electron acceptor of photosystem I. Biochim Biophys Acta - Rev Bioenerg 301:1–33. https://doi.org/10.1016/0304-4173(73)90010-4

Kimura A, Kitoh-Nishioka H, Aota T, et al. (2022) Theoretical Model of the Far-Red-Light-Adapted Photosystem I Reaction Center of Cyanobacterium *Acaryochloris marina* Using Chlorophyll d and the Effect of Chlorophyll Exchange. J Phys Chem B 126:4009–4021. https://doi.org/10.1021/acs.jpcb.2c00869

Kobayashi M, Akutsu S, Fujinuma D, et al. (2013) Physicochemical Properties of Chlorophylls in Oxygenic Photosynthesis — Succession of Co-Factors from Anoxygenic to Oxygenic Photosynthesis. In: Dubinsky Z (ed) Photosynthesis. InTech, pp 47–90

Kok B (1961) Partial purification and determination of oxidation reduction potential of the photosynthetic chlorophyll complex absorbing at 700 mμ. Biochim Biophys Acta 48:527–533. https://doi.org/10.1016/0006-3002(61)90050-6

Kramer H, Mathis P (1980) Quantum yield and rate of formation of the carotenoid triplet state in photosynthetic structures. Biochim Biophys Acta - Bioenerg 593:319–329. https://doi.org/10.1016/0005-2728(80)90069-9

Krasnovskiĭ AA (2004) Photodynamic activity and singlet oxygen. Biofizika 49:305–21

Krasnovsky AA (1982) Delayed fluorescence and phosphorescence of plant pigments. Photochem Photobiol 36:733–741. https://doi.org/10.1111/j.1751-1097.1982.tb09497.x

Krasnovsky AA (1994) Singlet molecular oxygen and primary mechanisms of photo-oxidative damage of chloroplasts. Studies based on detection of oxygen and pigment phosphorescence. Proc R Soc Edinburgh Sect B Biol Sci 102:219–235. https://doi.org/10.1017/S0269727000014147

Kühl M, Chen M, Ralph PJ, et al. (2005) A niche for cyanobacteria containing chlorophyll d. Nature 433:820–820. https://doi.org/10.1038/433820a

Kumazaki S, Abiko K, Ikegami I, et al. (2002) Energy equilibration and primary charge separation in chlorophyll d -based photosystem I reaction center isolated from *Acaryochloris marina*. FEBS Lett 530:153–157. https://doi.org/10.1016/S0014-5793(02)03446-4

Lathrop EJP, Friesner RA (1994) Vibronic mixing in the strong electronic coupling limit. Spectroscopic effects of forbidden transitions. J Phys Chem 98:3050–3055. https://doi.org/10.1021/j100062a050

Li Y, Scales N, Blankenship RE, et al. (2012) Extinction coefficient for red-shifted chlorophylls: Chlorophyll d and chlorophyll f. Biochim Biophys Acta - Bioenerg 1817:1292–1298. https://doi.org/10.1016/j.bbabio.2012.02.026

Lubitz W (2002) Pulse EPR and ENDOR studies of light-induced radicals and triplet states in photosystem II of oxygenic photosynthesis. Phys Chem Chem Phys 4:5539–5545. https://doi.org/10.1039/B206551G

Lubitz W, Lendzian F, Bittl R (2002) Radicals, Radical Pairs and Triplet States in Photosynthesis. Acc Chem Res 35:313–320. https://doi.org/10.1021/ar000084g

Mascoli V, Bersanini L, Croce R (2020) Far-red absorption and light-use efficiency trade-offs in chlorophyll f photosynthesis. Nat Plants 6:1044–1053. https://doi.org/10.1038/s41477-020-0718-z

Mathis P, Butler WL, Satoh K (1979) Carotenoid triplet state and chlorophyll fluorescence quenching in chloroplasts and subchloroplast particles. Photochem Photobiol 30:603–614. https://doi.org/10.1111/j.1751-1097.1979.tb07187.x

McLean MB, Sauer K (1982) The dependence of reaction center and antenna triplets on the redox state of Photosystem I. Biochim Biophys Acta - Bioenerg 679:384–392. https://doi.org/10.1016/0005-2728(82)90158-X

Mi D, Chen M, Lin S, et al. (2003) Excitation Dynamics in the Core Antenna in the Photosystem

I Reaction Center of the Chlorophyll d -Containing Photosynthetic Prokaryote *Acaryochloris marina*. J Phys Chem B 107:1452–1457. https://doi.org/10.1021/jp0268260

Mino H, Kawamori A, Aoyama D, et al. (2005) Proton ENDOR study of the primary donor P740+, a special pair of chlorophyll d in photosystem I reaction center of *Acaryochloris marina*. Chem Phys Lett 411:262–266. https://doi.org/10.1016/j.cplett.2005.06.033

Miyashita H, Ikemoto H, Kurano N, et al. (1996) Chlorophyll d as a major pigment. Nature 383:402–402. https://doi.org/10.1038/383402a0

Molotokaite E, Remelli W, Casazza AP, Zucchelli G, Polli D, Cerullo G, Santabarbara S (2017) Trapping Dynamics in Photosystem I-Light Harvesting Complex I of Higher Plants Is Governed by the Competition between Excited State Diffusion from Low Energy States and Photochemical Charge Separation. J. Phys. Chem. B 121: 9816–9830. https://doi.org/10.1021/acs.jpcb.7b07064

Müller MG, Niklas J, Lubitz W, Holzwarth AR (2003) Ultrafast Transient Absorption Studies on Photosystem I Reaction Centers from *Chlamydomonas reinhardtii*. 1. A New Interpretation of the Energy Trapping and Early Electron Transfer Steps in Photosystem I. Biophys J 85:3899–3922. https://doi.org/10.1016/S0006-3495(03)74804-8

Müller MG, Slavov C, Luthra R, Redding KE, Holzwarth AR (2010) Independent initiation of primary electron transfer in the two branches of the photosystem I reaction center. Proc. Natl. Acad. Sci. U. S. A. 107:4123–4128. https://doi.org/10.1073/pnas.0905407107

Nakamura A, Suzawa T, Kato Y, Watanabe T (2011) Species Dependence of the Redox Potential of the Primary Electron Donor P700 in Photosystem I of Oxygenic Photosynthetic Organisms Revealed by Spectroelectrochemistry. Plant Cell Physiol 52:815–823. https://doi.org/10.1093/pcp/pcr034

Neverov K V., Santabarbara S, Krasnovsky AA (2011) Phosphorescence study of chlorophyll d photophysics. Determination of the energy and lifetime of the photo-excited triplet state. Evidence of singlet oxygen photosensitization. Photosynth Res 108:101–106. https://doi.org/10.1007/s11120-011-9657-x

Niedzwiedzki DM, Blankenship RE (2010) Singlet and triplet excited state properties of natural chlorophylls and bacteriochlorophylls. Photosynth Res 106:227–238. https://doi.org/10.1007/s11120-010-9598-9

Nieuwenburg P, Clarke RJ, Cai Z-L, et al. (2007) Examination of the Photophysical Processes of

Chlorophyll d Leading to a Clarification of Proposed Uphill Energy Transfer Processes in Cells of A*caryochloris marina*¶. Photochem Photobiol 77:628–637. https://doi.org/10.1562/0031-8655(2003)0770628EOTPPO2.0.CO2

Nürnberg DJ, Morton J, Santabarbara S, et al. (2018) Photochemistry beyond the red limit in chlorophyll f–containing photosystems. Science (80-) 360:1210–1213. https://doi.org/10.1126/science.aar8313

Ohashi S, Miyashita H, Okada N, Iemura T, Watanabe T, Kobayashi M (2008)Unique photosystems in Acaryochloris marina. Photosynth Res (2008) 98:141–149. https://doi.org/10.1007/s11120-008-9383-1

Razeghifard MR, Chen M, Hughes JL, et al. (2005) Spectroscopic Studies of Photosystem II in Chlorophyll d -Containing *Acaryochloris marina*. Biochemistry 44:11178–11187. https://doi.org/10.1021/bi048314c

Renger T, Schlodder E (2008) The Primary Electron Donor of Photosystem II of the Cyanobacterium *Acaryochloris marina* Is a Chlorophyll d and the Water Oxidation Is Driven by a Chlorophyll a /Chlorophyll d Heterodimer. J Phys Chem B 112:7351–7354. https://doi.org/10.1021/jp801900e

Renger T, Schlodder E (2006) Modeling of Optical Spectra and Light Harvesting in Photosystem I. In: Golbeck JH (ed) Photosystem I. Advances in Photosynthesis and Respiration, vol 24. Springer Netherlands, Dordrecht, pp 595–610

Renger T, Trostmann I, Theiss C, et al. (2007) Refinement of a structural model of a pigment-protein complex by accurate optical line shape theory and experiments. J Phys Chem B 111:10487–10501. https://doi.org/10.1021/jp0717241

Rutherford AW, Sétif P (1990) Orientation of P700, the primary electron donor of Photosystem I. Biochim Biophys Acta - Bioenerg 1019:128–132. https://doi.org/10.1016/0005-2728(90)90133-O

Russo M, Petropoulos V, Molotokaite E, Cerullo G, Casazza AP, Maiuri M, Santabarbara S. (2020) Ultrafast excited-state dynamics in land plants Photosystem I core and whole supercomplex under oxidised electron donor conditions. Photosynth Res. 144:221-233. https://doi.org/10.1007/s11120-020-00717-y

Santabarbara S, Agostini A, Casazza AP, et al. (2015) Carotenoid triplet states in photosystem II: Coupling with low-energy states of the core complex. Biochim Biophys Acta - Bioenerg

1847:262–275. https://doi.org/10.1016/j.bbabio.2014.11.008

Santabarbara S, Agostini G, Casazza AP, et al. (2007) Chlorophyll triplet states associated with Photosystem I and Photosystem II in thylakoids of the green alga *Chlamydomonas reinhardtii*. Biochim Biophys Acta - Bioenerg 1767:88–105. https://doi.org/10.1016/j.bbabio.2006.10.007

Santabarbara S, Bailleul B, Redding K, et al. (2012) Kinetics of phyllosemiquinone oxidation in the Photosystem I reaction centre of *Acaryochloris marina*. Biochim Biophys Acta - Bioenerg 1817:328–335. https://doi.org/10.1016/j.bbabio.2011.10.003

Santabarbara S, Bordignon E, Jennings RC, Carbonera D (2002a) Chlorophyll triplet states associated with Photosystem II of thylakoids. Biochemistry 41:8184–8194. https://doi.org/10.1021/bi0201163

Santabarbara S, Carbonera D (2005) Carotenoid triplet states associated with the long-wavelength-emitting chlorophyll forms of photosystem I in isolated thylakoid membranes. J Phys Chem B 109:986–991. https://doi.org/10.1021/jp047077k

Santabarbara S, Casazza AP, Belgio E, et al. (2020) Light Harvesting by Long-Wavelength Chlorophyll Forms (Red Forms). In: Larkum A, Grossman A, Raven J (eds) Photosynthesis in Algae: Biochemical and Physiological Mechanisms. Advances in Photosynthesis and Respiration, vol 45. Springer, pp 261–297

Santabarbara S, Cazzalini I, Rivadossi A, et al. (2002b) Photoinhibition in vivo and in vitro Involves Weakly Coupled Chlorophyll–Protein Complexes‡¶. Photochem Photobiol 75:613. https://doi.org/10.1562/0031-8655(2002)075<0613:PIVAIV>2.0.CO;2

Santabarbara S, Galuppini L, Casazza AP (2010) Bidirectional Electron Transfer in the Reaction Centre of Photosystem I. J Integr Plant Biol 52:735–749. https://doi.org/10.1111/j.1744-7909.2010.00977.x

Santabarbara S, Heathcote P, Evans MCW (2005) Modelling of the electron transfer reactions in Photosystem I by electron tunnelling theory: The phylloquinones bound to the PsaA and the PsaB reaction centre subunits of PS I are almost isoenergetic to the iron–sulfur cluster FX. Biochim Biophys Acta - Bioenerg 1708:283–310. https://doi.org/10.1016/j.bbabio.2005.05.001

Santabarbara S, Jennings RC (2005) The size of the population of weakly coupled chlorophyll pigments involved in thylakoid photoinhibition determined by steady-state fluorescence

spectroscopy. Biochim Biophys Acta - Bioenerg 1709:138–149. https://doi.org/10.1016/j.bbabio.2005.06.001

Santabarbara S, Jennings RC, Carbonera D (2003) Analysis of photosystem II triplet states in thylakoids by fluorescence detected magnetic resonance in relation to the redox state of the primary quinone acceptor QA. Chem Phys 294:257–266. https://doi.org/10.1016/S0301-0104(03)00279-9

Santabarbara S, Neverov KV, Garlaschi FM, et al. (2001) Involvement of uncoupled antenna chlorophylls in photoinhibition in thylakoids. FEBS Lett 491:109–113. https://doi.org/10.1016/S0014-5793(01)02174-3

Schatz GH, Brock H, Holzwarth AR (1988) Kinetic and Energetic Model for the Primary Processes in Photosystem II. Biophys J 54:397–405. https://doi.org/10.1016/S0006-3495(88)82973-4

Schenderlein M, Çetin M, Barber J, et al. (2008) Spectroscopic studies of the chlorophyll d containing photosystem I from the cyanobacterium, *Acaryochloris marina*. Biochim Biophys Acta - Bioenerg 1777:1400–1408. https://doi.org/10.1016/j.bbabio.2008.08.008

Schiller H, Senger H, Miyashita H, et al. (1997) Light-harvesting in *Acaryochloris marina* - spectroscopic characterization of a chlorophyll d -dominated photosynthetic antenna system. FEBS Lett 410:433–436. https://doi.org/10.1016/S0014-5793(97)00620-0

Schlodder E, Çetin M, Eckert H-J, et al. (2007) Both chlorophylls a and d are essential for the photochemistry in photosystem II of the cyanobacteria, *Acaryochloris marina*. Biochim Biophys Acta - Bioenerg 1767:589–595. https://doi.org/10.1016/j.bbabio.2007.02.018

Searle GFW, Koehorst RBM, Schaafsma TJ, et al. (1981) Fluorescence detected magnetic resonance (FDMR) spectroscopy of chlorophyll-proteins from barley. Carlsberg Res Commun 46:183–194. https://doi.org/10.1007/BF02906496

Searle GFW, Schaafsma TJ (1992) Fluorescence detected magnetic resonance of the primary donor and inner core antenna chlorophyll in Photosystem I reaction centre protein: Sign inversion and energy transfer. Photosynth Res 32:193–206. https://doi.org/10.1007/BF00034795

Siefermann-Harms D (1987) The light-harvesting and protective functions of carotenoids in photosynthetic membranes. Physiol Plant 69:561–568. https://doi.org/10.1111/j.1399-3054.1987.tb09240.x

Sivakumar V, Wang R, Hastings G (2003) Photo-Oxidation of P740, the Primary Electron Donor in Photosystem I from *Acaryochloris marina*. Biophys J 85:3162–3172. https://doi.org/10.1016/S0006-3495(03)74734-1

Stoll S, Schweiger A (2006) EasySpin, a comprehensive software package for spectral simulation and analysis in EPR. J Magn Reson 178:42–55. https://doi.org/10.1016/j.jmr.2005.08.013

Telfer A (2014) Singlet Oxygen Production by PSII Under Light Stress: Mechanism, Detection and the Protective role of β-Carotene. Plant Cell Physiol 55:1216–1223. https://doi.org/10.1093/pcp/pcu040

Telfer A, Bishop SM, Phillips D, Barber J (1994) Isolated photosynthetic reaction center of photosystem II as a sensitizer for the formation of singlet oxygen. Detection and quantum yield determination using a chemical trapping technique. J Biol Chem 269:13244–13253. https://doi.org/10.1016/S0021-9258(17)36825-4

Tomo T, Allakhverdiev SI, Mimuro M (2011) Constitution and energetics of photosystem I and photosystem II in the chlorophyll d-dominated cyanobacterium *Acaryochloris marina*. J Photochem Photobiol B Biol 104:333–340. https://doi.org/10.1016/j.jphotobiol.2011.02.017

Tomo T, Kato Y, Suzuki T, et al. (2008) Characterization of Highly Purified Photosystem I Complexes from the Chlorophyll d-dominated Cyanobacterium *Acaryochloris marina* MBIC 11017. J Biol Chem 283:18198–18209. https://doi.org/10.1074/jbc.M801805200

Tomo T, Okubo T, Akimoto S, Yokono M, Miyashita H, Tsuchiya T, Noguchi T, Mimuro M (2007) Identification of the special pair of photosystem II in a chlorophyll d-dominated cyanobacterium. Proc Natl Acad Sci USA 104:7283–7288. https://doi.org/10.1073/pnas.0701847104

van Mieghem F, Brettel K, Hillman B, et al. (1995) Charge Recombination Reactions in Photosystem II. 1. Yields, Recombination Pathways, and Kinetics of the Primary Pair. Biochemistry 34:4798–4813. https://doi.org/10.1021/bi00014a038

Vass I, Styring S (1993) Characterization of chlorophyll triplet promoting states in photosystem II sequentially induced during photoinhibition. Biochemistry 32:3334–3341. https://doi.org/10.1021/bi00064a016

Viola S, Roseby W, Santabarbara S, et al. (2022) Impact of energy limitations on function and resilience in long-wavelength Photosystem II. Elife 11:. https://doi.org/10.7554/eLife.79890

Webber AN, Lubitz W (2001) P700: the primary electron donor of photosystem I. Biochim Biophys Acta - Bioenerg 1507:61–79. https://doi.org/10.1016/S0005-2728(01)00198-0

Witt H, Bordignon E, Carbonera D, et al. (2003) Species-specific differences of the spectroscopic properties of P700: Analysis of the influence of non-conserved amino acid residues by site-directed mutagenesis of photosystem I from *Chlamydomonas reinhardtii.* J Biol Chem 278:46760–46771. https://doi.org/10.1074/jbc.M304776200

Wolff C, Witt HT (1969) On Metastable States of Carotenoids in Primary Events of Photosynthesis. Zeitschrift für Naturforsch B 24:1031–1037. https://doi.org/10.1515/znb-1969-0818

Xu C, Zhu Q, Chen J, et al. (2021) A unique photosystem I reaction center from a chlorophyll d-containing cyanobacterium *Acaryochloris marina*. J Integr Plant Biol 63:1740–1752. https://doi.org/10.1111/jipb.13113

Zamzam N, Rakowski R, Kaucikas M, et al. (2020) Femtosecond visible transient absorption spectroscopy of chlorophyll-*f*-containing photosystem II. Proc Natl Acad Sci 117:23158–23164. https://doi.org/10.1073/pnas.2006016117

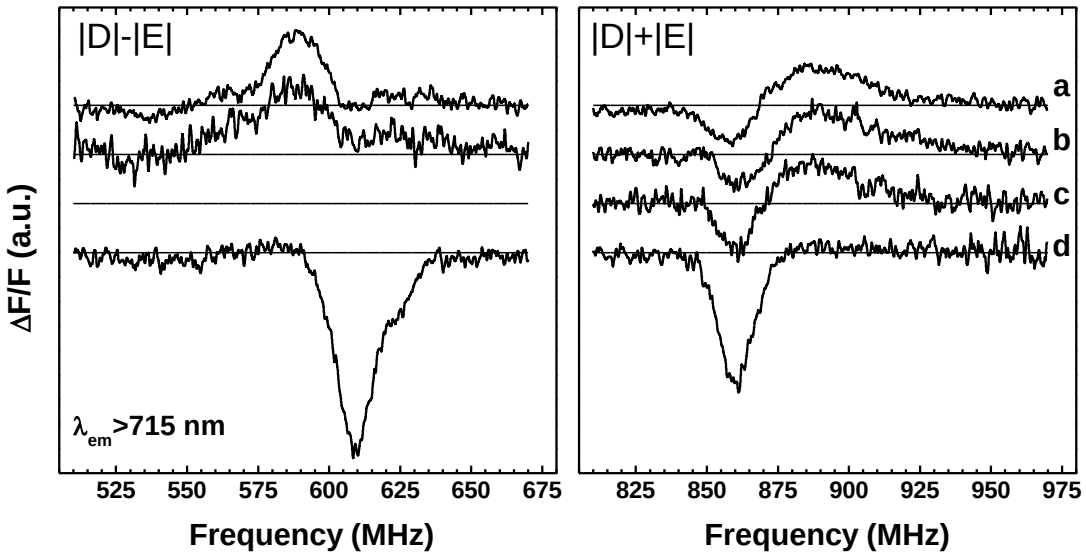

Figure 1. FDMR spectra of *A. marina* thylakoids recorded through a long-pass filter (λ>715 nm) in samples that were **a)** dark adapted for 15 min at RT or illuminated for 5 minutes at RT following incubation with **b)** 10 mM Asc **c)** 40 mM Asc **d)** 10 mM Asc and 80 μM TMPD. Measurement conditions: T,1.8 K; mw-amplitude modulation, 33.3 Hz; phase, -96°; scan rate, 2.5 MHz s^{-1}

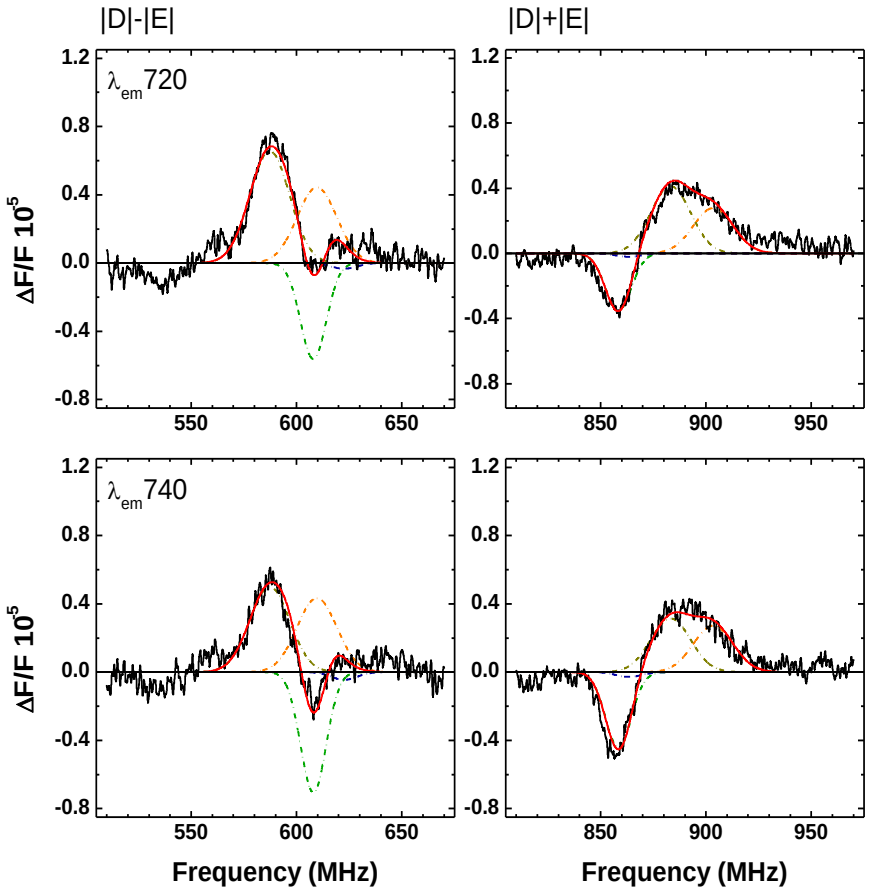

Figure 2. Decomposition of FDMR spectra in *A. marina* thylakoids, dark adapted at RT without the addition of reducing agents, at representative emission wavelengths. Black lines: experimental data; red lines: fitted spectra: dash-dotted lines: Gaussian sub-bands, orange (T_1), dark yellow (T_2), green (T_3), blue (T_4). Triplets T_1-T_4 are defined as in Table 1. Measurements conditions as in the legend of Figure 1.

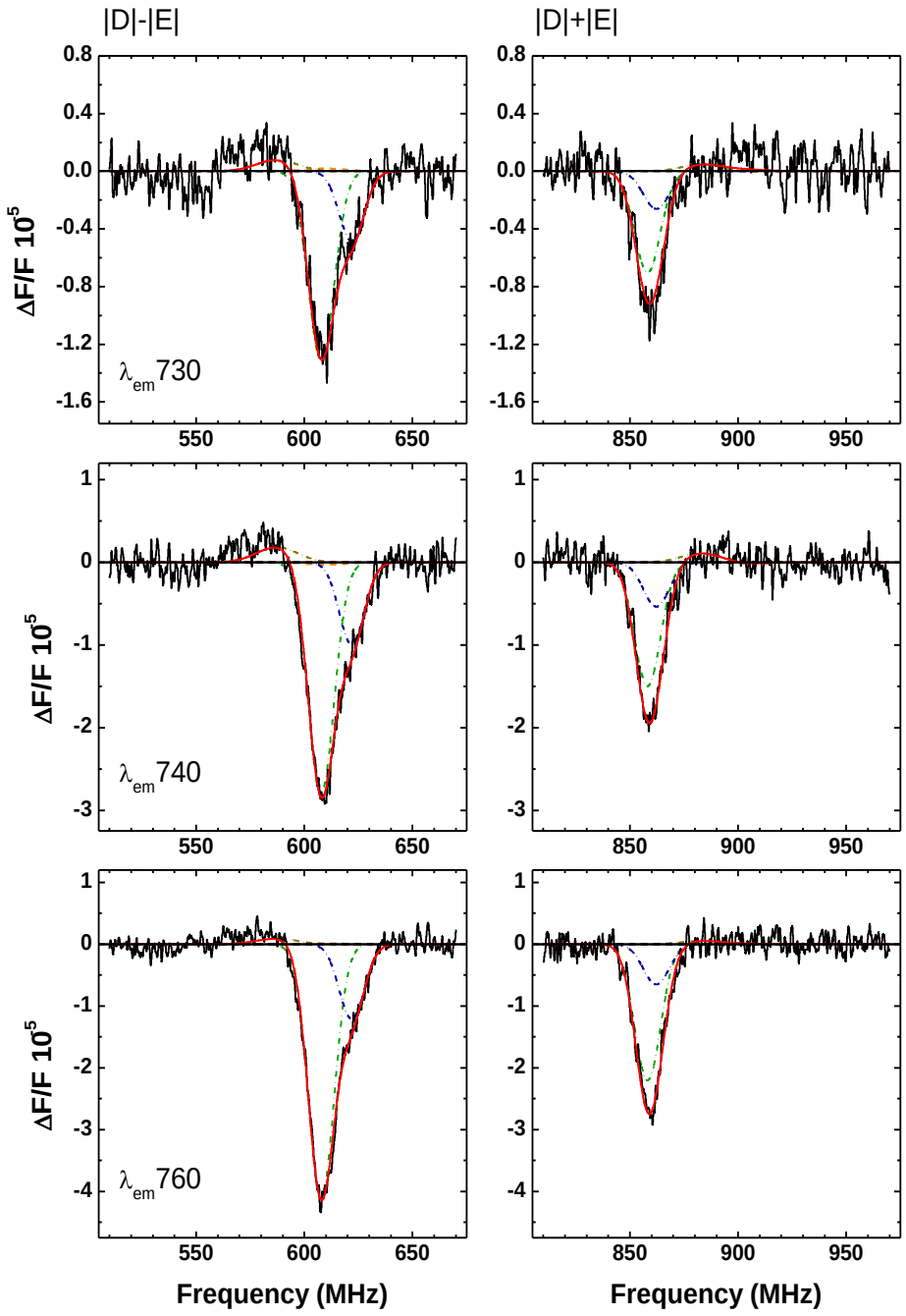

Figure 3. Decomposition of FDMR spectra in *A. marina* thylakoids, illuminated at RT in the presence of Asc (10 mM) and TMPD (80 μM), recorded at representative emission wavelengths. Black lines: experimental data; red lines: fitted spectra: dash-dotted lines: Gaussian sub-bands, orange (T_1), dark yellow (T_2), green (T_3), blue (T_4). Triplets T_1-T_4 are defined as in Table 1. Measurements conditions as in the legend of Figure 1.

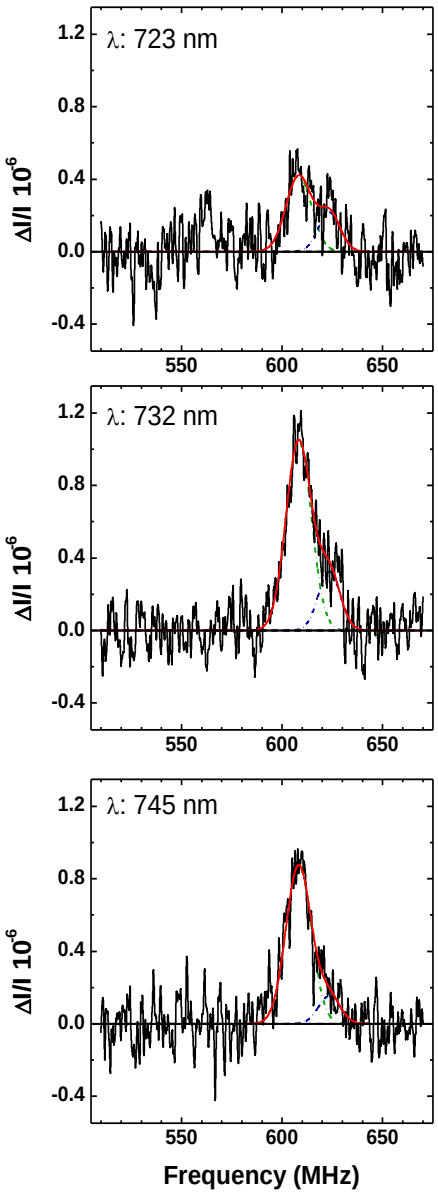

Figure 4. Decomposition of ADMR spectra in *A. marina* thylakoids, illuminated at RT in the presence of Asc (10 mM) and TMPD (80 μM), recorded at representative absorption wavelengths in the Chl *d* Q_y band. Black lines: experimental data; red lines: fitted spectra: dash-dotted lines: Gaussian sub-bands, orange (T_1), dark yellow (T_2), green (T_3), blue (T_4). Triplets T_1-T_4 are defined as in Table 1. Measurements conditions as in the legend of Figure 1, except that the phase was +80 °.

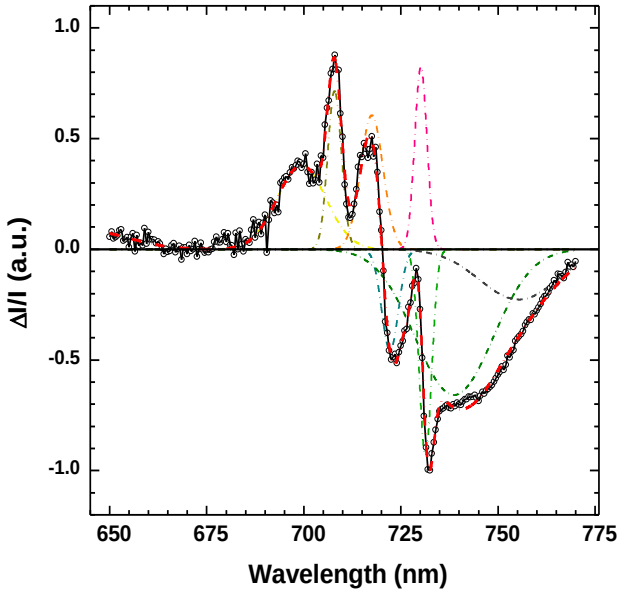

Figure 5. Microwave-induced TmS spectrum obtained upon excitation at 610 MHz, in *A. marina* thylakoids, illuminated at RT in the presence of Asc (10 mM) and TMPD (80 μM). Black lines and open symbols: experimental data; red lines: fitted spectra; dash-dotted lines: Gaussian sub-bands, with green shades representing singlet bleaching and yellow-orange shades describing the increase in absorption upon triplet population; the fit parameters are reported in Table 2. Measurements conditions as in the legend of Figure 1, except that the phase was +80° and the wavelength scan rate was 0.33 nm sec^{-1}.

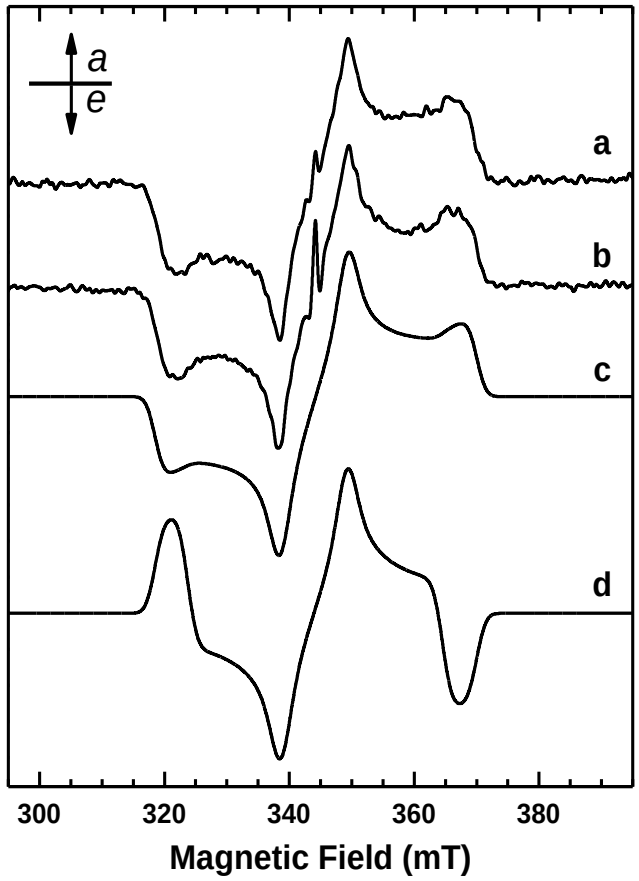

Figure 6. X-band triplet TR-EPR spectra of *A. marina* thylakoids that were **a)** dark adapted for 15 min at RT or **b)** illuminated at RT in the presence of Asc (10 mM) and TMPD (80 μM). The simulated **c)** ISC and **d)** recombination ^{3}Chl *d* spectra have been calculated using the following parameters: D = 25.8 mT, E = −5.35 mT, D strain = 2.5 mT, E strain = 1.5 mT, isotropic linewidth = 1.0 mT, microwave frequency 9.649 GHz. For the simulation of the **c)** ISC triplet, a polarization of (P_x:P_y:P_z) = (0.33:0.43:0.24) has been employed. The spectra have been vertically shifted for a better comparison. *a* = absorption, *e* = emission.